water

MDPI

Article

Techno-Economic Assessment and Process Design Considerations for Industrial-Scale Photocatalytic Wastewater Treatment

Hongliang Liu [1,*] and Mingxia Song [2]

[1] School of Innovation and Entrepreneurship, Nanjing University of Industry Technology, Nanjing 210023, China
[2] Jiangsu Key Laboratory of New Energy Devices and Interface Science, School of Chemistry and Materials Science, Nanjing University of Information Science and Technology, Nanjing 210044, China; smx839@nuist.edu.cn
* Correspondence: 2020101090@niit.edu.cn

Abstract

Industrial deployment of photocatalysis for recalcitrant wastewater treatment remains constrained by economic uncertainty and scale-up limitations. This study first reviews the current technological routes and application status of photocatalytic processes and then addresses the key obstacles through a quantitative techno-economic assessment (TEA) of a full-scale (10,000 m^3/d) photocatalytic wastewater treatment plant. A process-level model integrating mass- and energy-balance calculations with equipment sizing was developed for a 280 kW UVA-LED reactor using Pt/TiO_2 as the benchmark catalyst. The framework quantifies capital (CAPEX) and operating (OPEX) expenditures and evaluates the overall economic performance of the photocatalytic treatment system. Sensitivity analysis reveals that the catalyst replacement interval and electricity tariffs are the principal economic bottlenecks, whereas improvements in catalyst performance alone provide limited cost leverage. Furthermore, the analysis indicates that supportive policy mechanisms such as carbon-credit incentives and electricity subsidies could substantially enhance economic feasibility. Overall, this work establishes a comprehensive integrated TEA framework for industrial-scale photocatalytic wastewater treatment, offering actionable design parameters and cost benchmarks to guide future commercialization.

Keywords: photocatalysis; techno-economic analysis; industrial wastewater treatment; cost benchmarking

Check for updates

Academic Editor: Chih-Huang Weng

Received: 12 November 2025
Revised: 11 January 2026
Accepted: 12 January 2026
Published: 14 January 2026

Copyright: © 2026 by the authors. Licensee MDPI, Basel, Switzerland. This article is an open access article distributed under the terms and conditions of the Creative Commons Attribution (CC BY) license.

1. Introduction

Water pollution control is a key issue on the global sustainable development agenda. It involves technology pathways crucial for ecological safety and the stability and resilience of economic systems [1]. The acceleration of industrialization and the emergence of new pollutants such as antibiotics, endocrine disruptors, and per- and polyfluoroalkyl substances [2,3], pose challenges to traditional wastewater treatment technologies in terms of efficiency limits and environmental risks. There is an urgent need for technological innovation to disrupt the detrimental cycle of pollution transfer.

Biological methods, such as the activated sludge process and the Anaerobic–Anoxic–Oxic (A^2/O) process, are fundamental in current wastewater treatment systems due to their microbial degradation capabilities and cost-effectiveness for low- to medium-strength wastewater [3]. However, these methods exhibit limited resilience to fluctuations in influent quality and shock loads, hindering long-term maintenance of consistently low total nitrogen

effluent concentrations [4]. Moreover, the substantial production of excess sludge poses a significant environmental challenge [5], as this sludge, which contains heavy metals and pathogens, can emit methane when landfilled and poses a risk of dioxin formation when incinerated without adequate emission controls [6]. While advanced anaerobic digestion can facilitate biogas recovery, it requires a substantial capital investment and may lead to the concentration of heavy metals and recalcitrant organic pollutants, thereby exacerbating pollution transfer [7].

Photocatalysis exhibits significant disruptive potential in wastewater treatment compared to conventional technologies due to its unique free-radical-driven mineralization mechanism [8–11]. This technology can efficiently degrade organic matter into CO_2 and H_2O through chain oxidation by photogenerated free radicals ($\cdot OH$,$\cdot O_2^-$) [12], as illustrated in Figure 1. Theoretically, this approach overcomes the challenges associated with traditional methods, such as sludge disposal and the generation of toxic by-products [13,14]. In the treatment of refractory industrial wastewater, particularly with complex pollutants like polycyclic aromatic hydrocarbons and azo dyes, solar-driven photocatalysis allows for reduced energy costs and thorough mineralization [15].

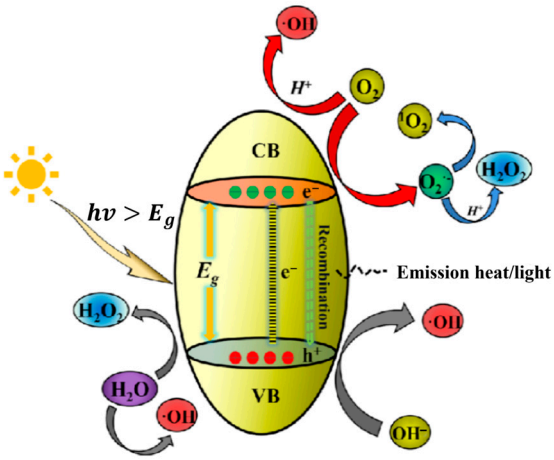


Figure 1. The photogenerated carriers and reactive oxygen species formation process [12].

However, practical implementation faces obstacles, including rapid recombination of photogenerated electron–hole pairs, low quantum efficiency (QE), a limited catalyst replacement interval, and reliance on noble metal catalysts. These factors result in high energy costs that hinder economic feasibility and widespread adoption [16]. Against this backdrop, a critical knowledge gap persists: the lack of a rigorous techno-economic benchmark for standalone photocatalytic treatment systems. While recent reviews highlight promising hybrid configurations (e.g., photocatalysis coupled with biological or membrane processes) [17,18], such integrations often obscure the intrinsic cost drivers and performance limits of the photocatalytic core itself. To enable transparent evaluation and targeted innovation, this study establishes a comprehensive techno-economic baseline for an industrial-scale, standalone Pt/TiO_2 photocatalytic system, focusing exclusively on its direct treatment capability without auxiliary processes.

This granular assessment is critical because the persistent gap between photocatalysis's theoretical promise and its real-world deployment stems not only from a scarcity of novel materials, but also from an insufficient understanding of its intrinsic economic viability under true industrial operating conditions.

This discrepancy between the technology's potential and its practical application underscores a crucial yet often neglected aspect of environmental technology innovation: the imperative to concurrently enhance photocatalytic efficiency and control life-cycle

costs to facilitate the transition of photocatalytic technologies from laboratory concept to industrial implementation.

2. Photocatalytic Technology and Economic Bottlenecks

Photocatalytic water treatment has progressed from laboratory proof-of-concept to engineering-scale pilots, yet its industrialization trajectory varies significantly across applications due to persistent technical and economic challenges [9]. This section reviews the primary application domains and analyzes the key limitations that constrain commercial deployment. These insights form the technological basis for the techno-economic model developed in this study.

2.1. Application Domains: From Broad Potential to Context-Specific Challenges

2.1.1. Industrial Wastewater: The Core Battleground and the Efficacy Gap

Industrial wastewater is a major global source of water pollution, with annual discharges reaching approximately 380 trillion liters, containing an estimated 300–400 million tons of untreated hazardous contaminants, such as persistent organic pollutants, toxic dyes, and heavy metals, posing serious threats to ecosystems and human health [19,20]. Compared with conventional treatment methods like chlorination and adsorption, photocatalysis is increasingly recognized as a promising alternative due to its operation under ambient conditions, low energy requirements, and minimal generation of secondary pollution [21]. Recent research has focused on developing advanced photocatalysts to enhance activity and stability. For example, platinum-decorated TiO_2 (Pt/TiO_2) improves charge separation, enabling rapid degradation of organic dyes under UV and visible light [22]. Polymeric carbon nitride (g-C_3N_4), defective polymeric carbon nitride, and g-C_3N_4/metal oxide composites have emerged as promising materials for enhancing photocatalytic performance due to their advantages in improving charge separation efficiency and extending the absorption range of visible light to longer wavelengths [8,11,23]. Transition metal dichalcogenides, such as MoS_2/WS_2 heterostructures, show strong reusability and resistance to deactivation over multiple cycles [24]. Although these materials demonstrate significant laboratory-scale potential, their real-world applicability in complex industrial effluents remains constrained by cost, scalability, and long-term stability challenges. Crucially, the efficacy gap stems not only from economic factors but also from fundamental incompatibilities between raw industrial wastewater matrices and photocatalytic reaction requirements [25]. The practical deployment of standalone solar photocatalysis is inherently constrained by feedwater quality. High organic loads diminish treatment efficiency through excessive scavenging of photogenerated radicals [26], while suspended solids and colored compounds significantly attenuate light penetration due to absorption and scattering [27], collectively necessitating influent streams with moderate organic content and low turbidity. Furthermore, common inorganic anions (e.g., Cl^-, HCO_3^-, PO_4^{3-}) can interfere with reactive oxygen species or compete for active sites on the catalyst surface, thereby reducing degradation kinetics [27]. Critically, wastewaters containing interfering cations and compounds such as heavy metals (e.g., Hg^{2+}, Pb^{2+}) and other catalyst poisons may induce deactivation of photocatalysts, substantially shortening operational lifetime [26]. Consequently, effective application typically requires pre-treated effluents rather than raw industrial discharges. This necessity also applies to organic loading: recent reviews indicate that influent COD above approximately 300–400 mg/L leads to excessive scavenging of photogenerated radicals and markedly reduced degradation efficiency [26], while successful pilot-scale solar photocatalytic systems commonly precondition wastewater to COD levels below 400 mg/L to maintain practical reaction rates and catalyst stability [28]. Accordingly, this study adopts a baseline scenario with COD $\approx$ 300 mg/L, low turbidity, and absence of strong catalyst poisons, which is a

water quality profile that defines a technically feasible operating window for Pt/TiO_2-based solar photocatalysis under current engineering constraints [26,28].

2.1.2. Municipal and Agricultural Wastewater: Targeted Removal and the Need for System Integration

Municipal wastewater, derived from domestic sewage, industrial discharges, and stormwater runoff, contains complex mixtures of pollutants. Agricultural wastewater often includes high levels of organic compounds, pathogens, and antibiotic residues. Pharmaceuticals and pesticides in both streams raise concerns regarding disease transmission and broader environmental and public health risks [21,29]. In this context, photocatalysis offers unique advantages by simultaneously degrading antibiotic residues and inactivating microorganisms. While standalone systems show moderate activity, their efficiency improves significantly when integrated with biological processes. For instance, integration with a moving bed biofilm reactor (MBBR) has been shown to enhance pharmaceutical removal to ~96% in municipal and ~99% in industrial wastewater [21]. Similarly, BiOBr/TiO_2 nanotubes achieve 88.1% degradation of tetracycline hydrochloride (outperforming pure TiO_2) due to improved charge separation and adsorption capacity [10].

2.2. Technology Pathways: Balancing Material Performance and Process Economics

Despite the inherent benefits of utilizing solar energy directly (consuming low energy and producing minimal secondary pollution), photocatalysis encounters two primary obstacles: inadequate light absorption, especially in the visible spectrum, and rapid recombination of electron–hole pairs generated during the process. Current industrial efforts predominantly revolve around catalysts based on TiO_2, employing a variety of methods to overcome these hurdles.

2.2.1. The Modified TiO_2 Route: High Activity at the Expense of Cost and Complexity

The modification of TiO_2 through non-metal doping (e.g., C, N, F) [30–32], or noble metal deposition (e.g., Pt, Au, Ag) [33], illustrated in Figure 2, is the most widely used approach to improve visible-light absorption and QE. To facilitate catalyst recovery, immobilization on supports such as ceramics, zeolites, or bentonite is commonly employed, though this may reduce the active surface area and hinder mass transfer. For example, a Pt-doped TiO_2/MIL-125 composite achieved 98.97% degradation of Rhodamine B at a concentration of 5 mg/L under a 40 W UV lamp (wavelength 254 nm) after 30 min [34]. The Schottky barrier formed by Pt nanoparticles on the surface of the M-Pt-TiO_2 catalyst greatly enhances the photocatalytic reaction efficiency by inhibiting the recombination of photogenerated electron–hole pairs. Despite its high activity, the use of noble metals and complex synthesis routes raises concerns regarding cost and scalability.

This approach encounters a structural economic paradox: performance improvements achieved via noble metals and complex modifications substantially increase the initial and production costs. Whether these enhancements yield net economic benefits hinges on system integration, operational lifetime, and catalyst recyclability. In practice, the value of higher activity must be assessed not merely by energy savings, but by its ability to offset greater capital intensity, operational complexity, and challenges in end-of-life catalyst recovery.

2.2.2. The Non-Noble-Metal Catalyst Route: A Cost-Oriented, Sustainable Pathway

To overcome cost limitations, alternative pathways utilizing g-C_3N_4 and carbonaceous materials have emerged [35,36]. Due to its stable physicochemical properties, suitable bandgap (~2.7 eV), and ease of preparation, g-C_3N_4 exhibits favorable visible-light absorption [37]. Constructing Z-scheme TiO_2/g-C_3N_4 heterojunctions promotes charge separation

and boosts activity. For example, Z-scheme composites achieved up to 95% degradation of rhodamine B, significantly outperforming the single components. The mechanism is illustrated in Figure 3 [38].

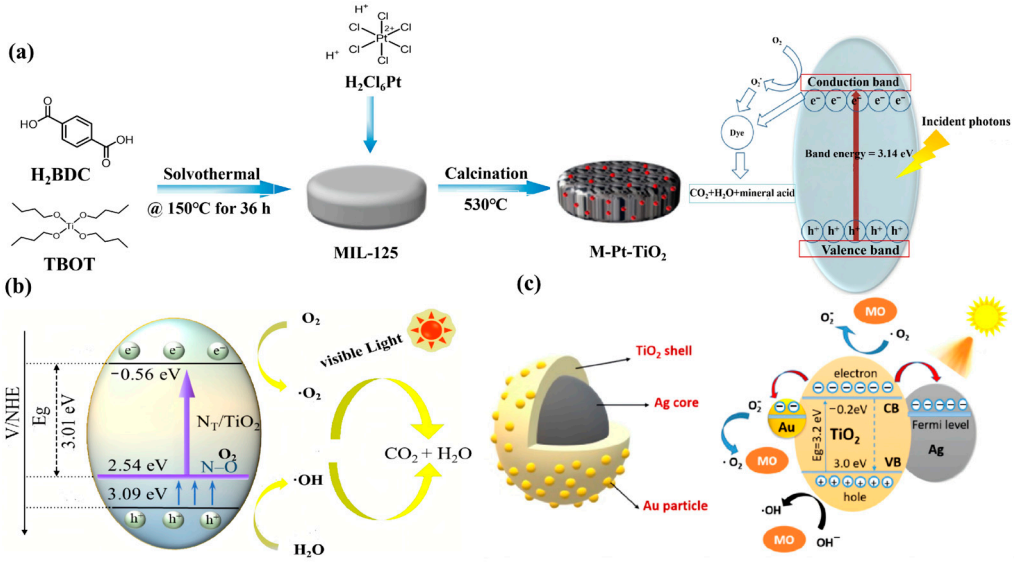


Figure 2. (**a**) Schematic representation and suggested mechanism for the photocatalytic degradation of RhB by M-Pt-TiO_2 [34]; (**b**) Schematic diagram of the photocatalytic mechanism of the N_T/TiO_2 photocatalyst [32]; (**c**) Schematic diagram and scheme of the proposed photocatalytic mechanism of the Au-Ag@TiO_2 ternary core–shell nanostructure [33].

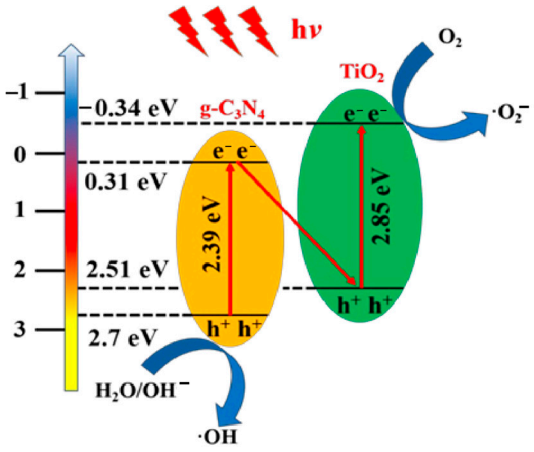


Figure 3. Possible mechanism of Z-scheme TiO_2/g-C_3N_4 heterojunction under irradiation [38].

The primary advantage of this approach lies in its ability to reduce reliance on noble metals, addressing the issue of high material costs. However, a significant challenge arises in balancing stability with long-term operational costs. Non-metal catalysts, particularly g-C_3N_4, are susceptible to photocorrosion and structural degradation in practical wastewater settings, necessitating frequent replacement. Consequently, the elevated operational and maintenance costs (e.g., material replacement, downtime) may negate the initial cost savings over the system's lifetime. Therefore, for these materials to be commercially feasible, they must exhibit enhanced long-term stability while preserving their cost-effectiveness.

2.2.3. The Multi-Technology Integration Route: A System-Engineering Approach to Single-Route Constraints

Building on the observation in Section 2.1.2 that photocatalytic efficiency improves markedly when coupled with biological processes, multi-technology integration has been

proposed as a potential system-engineering strategy to address the inherent trade-offs between performance, cost, and stability in standalone photocatalytic systems.

Rather than pursuing a single optimal catalyst, this approach leverages the complementary strengths of distinct unit processes to address refractory pollutants more holistically. Typical configurations couple photocatalysis with biological treatment systems such as membrane bioreactors (MBRs) or MBBRs [39–42] (illustrated in Figure 4). For instance, López et al. [43] demonstrated that solar photocatalytic pretreatment of pesticide-laden wastewater increased the BOD_5/COD ratio from less than 0.1 to greater than 0.4, enabling subsequent biological units to achieve over 90% COD removal while mitigating membrane fouling, which represents a clear pathway to reduce aeration energy consumption and maintenance. Similarly, Zhang et al. [42] reported a simultaneous photocatalysis-activated sludge system in which microbial degradation of photocatalytic intermediates suppressed electron–hole recombination, thereby enhancing decontamination efficiency by 30–50% and improving apparent quantum efficiency, ultimately reducing reliance on chemical oxidants. This integration route enables a structural shift in operating costs: photocatalytic pretreatment can lower aeration demand, minimize membrane-fouling-related expenditures, and avoid reagent costs associated with other advanced oxidation processes (e.g., Fenton oxidation, ozonation). In essence, it substitutes a higher upfront capital investment for additional reactors, a larger footprint, and advanced control systems in exchange for long-term operational savings. However, as Lu et al. [44] emphasized, such coupling introduces significant complexity and operational risks. Fluctuations in the quality of photocatalytic effluent and the transient toxicity of intermediate byproducts (e.g., aldehydes, short-chain carboxylic acids) may inhibit microbial activity and destabilize biological performance. These uncertainties necessitate more rigorous design, commissioning, and real-time monitoring compared to single-technology systems. Consequently, while promising high-strength industrial wastewater applications, the economic feasibility of integrated routes remains highly site-specific and warrants pilot-scale validation prior to full-scale deployment.

2.3. Research Gap and This Study's Focus

Although substantial progress has been achieved in photocatalyst design and process integration, systematic techno-economic evaluations that quantitatively examine the financial viability of industrial-scale photocatalytic systems and pinpoint the dominant cost drivers under realistic operating conditions remain limited [45].

Among the available options, Pt/TiO_2-based systems stand out as one of the most technologically mature and well-studied platforms for industrial wastewater treatment [46]. Their well-defined performance characteristics, standardized synthesis procedures, and demonstrated scalability make them an ideal benchmark for techno-economic analysis. Assessing this reference system not only clarifies its current economic feasibility but also enables meaningful comparison with emerging, lower-cost alternatives, thereby guiding long-term R&D priorities.

To fill this gap, the present study develops a process-based cost model integrated with a dynamic net present value (NPV) framework, using the Pt/TiO_2 system as a representative high-performance pathway. Unlike conventional life-cycle cost analysis (LCCA) or static NPV approaches that often rely on aggregated cost categories and fixed component lifetimes [47], our dynamic NPV framework explicitly embeds time-resolved engineering realities into a discounted cash flow model calibrated with real-world market data (Section 3.1). Specifically, it accounts for (i) discrete equipment and catalyst replacement events at defined intervals (e.g., Year 4 and Year 8); (ii) catalyst lifetime as a function of feedwater quality constraints (COD $\approx$ 300 mg/L, low turbidity, absence of poisons; Section 2.1.1); and (iii) end-of-life platinum recovery as a creditable revenue stream. By

directly linking technical performance boundaries to financial outcomes, the model enables rigorous sensitivity and break-even analyses that reflect actual operational risks and economic trade-offs. To our knowledge, this is among the first techno-economic assessments of photocatalytic wastewater treatment to integrate such granular, time-dependent cost drivers within an NPV framework under explicitly defined feasibility limits. This approach extends conventional LCCA practice by embedding operational realism into financial evaluation, as further contextualized against typical LCA/LCCA methodologies in Appendix C (Table A7).

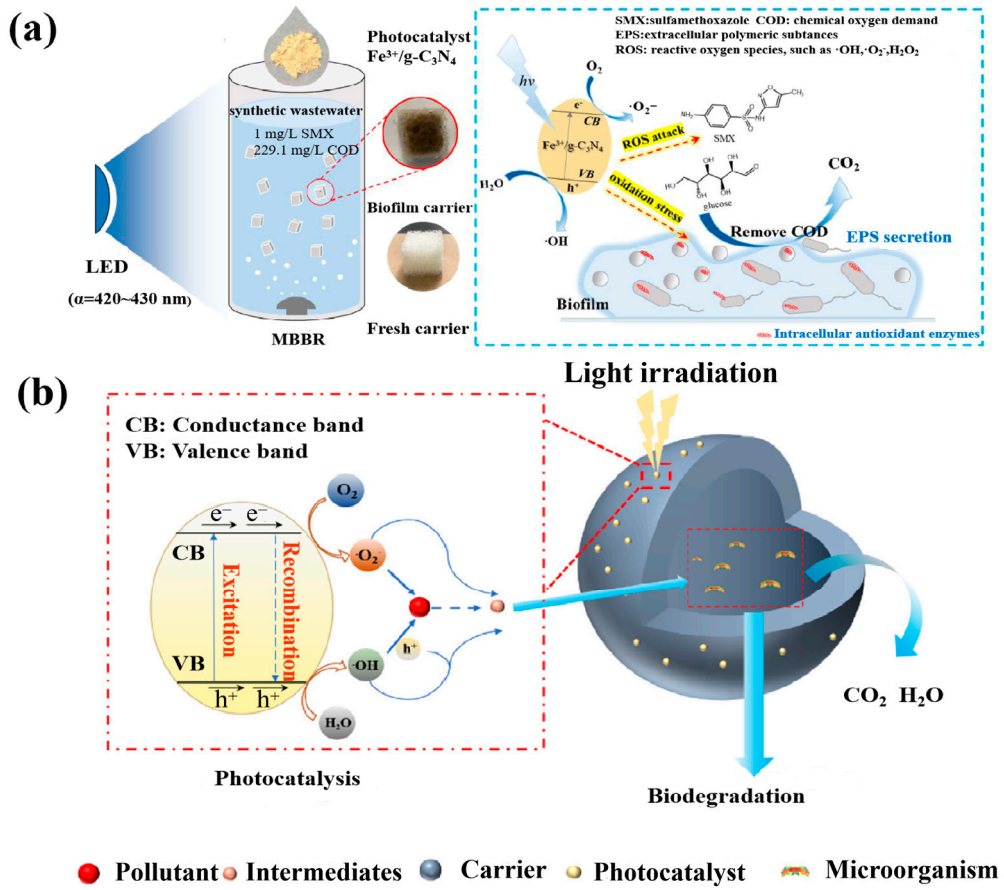


Figure 4. (**a**) Schematic diagram of an integrated photocatalysis and MBBR system in treating synthetic wastewater [39]; (**b**) Schematic diagram illustrating the principle of intimately coupling photocatalysis and biological (ICPB) system [41].

The model quantitatively evaluates the economic feasibility under current technological and market conditions, analyzes the sensitivity of profitability to key parameters such as catalyst cost, replacement interval, and electricity price, and provides actionable insights for strategic development, including both incremental improvements to existing systems and potential transitions toward non-noble-metal catalysts.

3. Cost–Benefit Analysis

3.1. NPV Analysis of the Modified TiO_2 Technology

This study focuses on evaluating the financial feasibility of the Pt/TiO_2-based photocatalytic pathway by developing a dynamic NPV model to assess project viability under specific techno-economic constraints.

3.1.1. Model Framework and Key Parameter Assumptions

To establish a realistic and transparent techno-economic model, the system design is based on a full-scale Pt/TiO_2-based photocatalytic wastewater treatment process. The economic analysis is based on a pre-treated industrial effluent stream with a moderate organic load (COD ≈ 300 mg/L), low turbidity, and the absence of known platinum poisons (e.g., sulfides, cyanides, or heavy metals). All financial projections in Tables 1–5, including treatment capacity, revenue, operating costs, and catalyst replacement schedules, are strictly conditional on this influent quality profile. The process flow diagram (PFD) and defined system boundaries are illustrated in Figure 5. The system is divided into four major subsystems: (1) Pretreatment, (2) Core Photocatalytic Reaction, (3) Post-treatment, and (4) Utilities. The boundary encompasses all material and energy flows relevant to cost analysis, including chemical inputs, electricity consumption, catalyst replacement, and platinum (Pt) recovery.

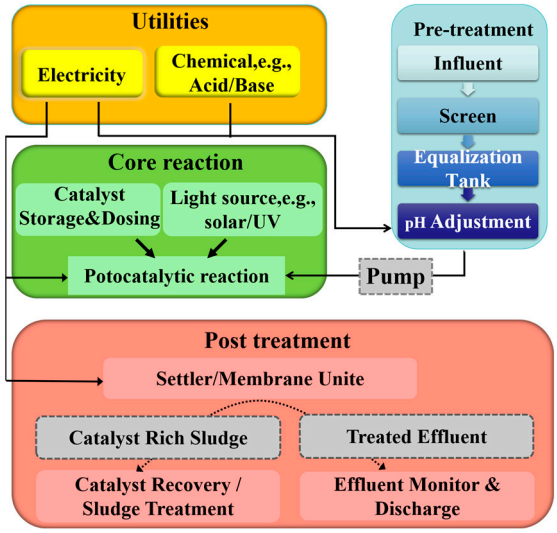


Figure 5. PFD and system boundaries of the Pt/TiO_2-based photocatalytic wastewater treatment system used for techno-economic analysis.

The project evaluation period is set at 10 years with a wastewater treatment capacity of 10,000 m^3/d. Key parameter assumptions for constructing the NPV model are established based on market research, vendor consultations, engineering cost estimates, and governmental regulations. Full details of the base-case parameters and data sources are provided in Appendix A (Table A5). All monetary values are expressed in the constant of 2024 Chinese yuan (CNY) without inflation adjustment. The key parameters for the annual cost–benefit calculation are summarized in Table 1.

Table 1. Annual Cost–Benefit Calculation for the Pt/TiO_2 Technology under the Base Scenario. (Unit: million CNY).

Items	Calculation Basis/Formula	Amount (Million CNY)
Operating Revenue	10,000 m^3/d × 365 d × 3.0 CNY/m^3	10.95
Less: Operating Costs		
Annual Electricity Cost	Based on time-of-use tariff calculation	1.56
Annual Labor Cost	Project-specific estimation	0.48
Annual Maintenance Cost	Project-specific estimation	0.30
Total Operating Costs		2.34

Table 1. *Cont.*

Items	Calculation Basis/Formula	Amount (Million CNY)
Less: Annual Depreciation and Amortization (D&A)	Prorated from fixed assets over useful life (updated for lower Pt CAPEX)	3.37
Earnings Before Tax (EBT)	Operating Revenue—Operating Costs—D&A	5.24
Less: Corporate Income Tax (25%)	EBT × 25%	1.31
Net Profit After Tax	EBT—Income Tax	3.93
Plus: Annual Depreciation (D&A)	Add-back of non-cash expense	3.37
Net Operating Cash Flow (NCF)	Net Profit After Tax + D&A	7.30

Note: The treatment fee of 3.00 CNY/m^3 assumes consistent compliance with discharge standards (e.g., COD < 50 mg/L [48]).

3.1.2. Life-Cycle Cash Flow Modeling and NPV Analysis Considering Equipment Replacement and Salvage Values

While the annual cost–benefit calculation in Table 1 provides a snapshot of operational profitability, a comprehensive assessment of the project's financial viability requires a dynamic analysis that accounts for major capital expenditures and recoveries throughout its entire lifetime. To accurately depict this, we construct a detailed annual cash flow model that explicitly factors in planned capital replacements, the final salvage value of fixed assets, and the recovery of working capital. These considerations are integrated into a discounted cash flow framework to calculate the base-case NPV. The resulting cash flow schedule is outlined in Table 2.

Table 2. Calculation of Net Cash Flows at Key Points in the Project Life-cycle (Unit: million CNY).

Year	Category	Calculation Items	Amount (Million CNY)
0	Total Initial Investment	Reactor (8.0) + LED (8.0) + Carrier (6.0) + Catalyst (4.43) + Working Capital (4.0)	–30.43
1–3, 5–7, 9	Normal Year NCF	Net Profit After Tax (3.93) + D&A (3.37)	7.30
4	Year 4 NCF	Normal Year NCF (7.30) − Catalyst Replacement (4.43) + Pt Recovery (1.56)	4.43
8	Year 8 NCF	Normal Year NCF (7.30) − Catalyst Replacement (4.43)—LED Replacement (8.0) + Pt Recovery (1.56)	–3.57
10	Terminal Year NCF	Normal Year NCF (7.30) + Working Capital Recovery (4.0) + Salvage Value (1.40) + Pt Recovery (1.56)	14.26

Note: Conservatively, the catalyst replacement cost was assumed to equal the full catalyst system investment (4.43 million CNY) every four years, although in practice only a portion of the modules may require renewal. For the calculation of Pt recovery, refer to Appendix B.

Based on the cash flow timeline above, the NPV is calculated using the formula:

$$NPV = \sum_{t=0}^{n} \frac{CF_t}{(1+i)^t} = \frac{CF_0}{(1+i)^0} + \frac{CF_1}{(1+i)^1} + \frac{CF_2}{(1+i)^2} + \ldots + \frac{CF_{10}}{(1+i)^{10}} \quad (1)$$

Where *CFt* is the net cash flow in year t, i is the discount rate (10%), and n is the total project duration (10 years). The present value of cash flows for each year and the summary calculation are shown in Table 3.

The calculation yields an NPV of 9.08 million CNY under the base scenario (4-year catalyst replacement interval, 10% discount rate). This positive result indicates that the project is financially viable. It not only fully covers the initial investment and all reinvestments throughout its life-cycle but also generates excess economic returns that exceed the cost of capital (i.e., the 10% discount rate).

Table 3. NPV Calculation under the Base Scenario (Unit: million CNY).

Year (t)	Net Cash Flow (CF_t)	Discount Factor ($1/(1 + 0.1)^t$)	Present Value (Million CNY)
0	–30.43	1.000	–30.43
1	7.30	0.909	6.64
2	7.30	0.826	6.03
3	7.30	0.751	5.48
4	4.43	0.683	3.03
5	7.30	0.621	4.54
6	7.30	0.564	4.12
7	7.30	0.513	3.74
8	–3.57	0.467	–1.67
9	7.30	0.424	3.10
10	14.26	0.386	5.50
Total NPV			9.08

3.2. Integrated Interpretation of Economic Drivers

The base-case NPV of 9.08 million CNY establishes the financial viability of the Pt/TiO_2 photocatalytic system under the stated assumptions. To assess the robustness of this positive outcome and identify key project risks, we conduct a comprehensive sensitivity analysis. This integrated interpretation combines insights from both sensitivity and break-even evaluations to elucidate the interdependent dimensions of economic risk and their implications for strategic technology development. Critically, this sensitivity analysis presumes operation within the technically feasible window defined in Section 2.1.1.

Detailed sensitivity results are provided in Table 4, and the break-even thresholds for key parameters are summarized in Table 5.

Table 4. Single-Factor Sensitivity Analysis of Key Parameters.

Parameter	Scenario	Factor Value/Impact	NPV (Million CNY)	NPV Change (Million CNY)	NPV Change Rate (%)
Base NPV	–	i = 10%	9.08	0	0
Catalyst Replacement Interval	Pessimistic	3 years (replace at yr 3, 6, 9), including Pt recovery revenue	3.43	–5.65	–62.2%
	Extremely Pessimistic	2 years (replace at yr 2, 4, 6, 8, 10), including Pt recovery revenue *	–3.37	–12.45	–137.10%
Discount Rate (i)	+20%	12%	5.88	–3.20	–35.20%
	+50%	15%	1.82	–7.26	–79.90%
Wastewater Treatment Fee	−10%	2.70 CNY/m^3	4.61	–4.47	–49.20%
	+ 10%	3.30 CNY/m^3	13.55	+4.47	+49.20%
Platinum (Pt) Price	+50%	362.85 CNY/g	6.84	–2.24	–24.70%
	+104%	495 CNY/g	0	–9.08	–100%
QE	−10%	10% deviation from base QE	8.38	–0.70	–7.70%
	+10%	10% deviation from base QE	9.78	0.70	7.70%
Influent COD Concentration	−20%	240 mg/L	10.97	+1.89	+20.8%
	+20%	360 mg/L	3.20	−5.88	–64.8%
LED Module Post-Replacement Efficiency	Pessimistic	90% of initial photon output after each replacement	9.04	−0.04	–0.44%
	Extremely Pessimistic	80% of initial photon output after each replacement	8.99	−0.09	–0.99%

Note: * The 2-year replacement scenario approximates operational conditions where Pt-based co-catalysts suffer rapid deactivation from residual sulfides, cyanides, or heavy metals, common constituents in untreated or poorly pretreated industrial streams. The COD sensitivity analysis assumes pseudo-first-order photocatalytic kinetics with a fixed effluent target (COD < 50 mg/L), linking influent concentration variations to electricity consumption via the logarithmic relationship between organic load and the required treatment time.

Table 5. Break-even Analysis of Key Parameters (NPV = 0 at Break-even Point; Unit: million CNY).

Factor	Base Value	Break-Even Value	Change from Base to Break-Even
Catalyst Replacement Interval	4 years	3.08 years	23.0% shorter
Discount Rate (i)	10%	15.9%	59.0% higher
Wastewater Treatment Fee	3.00 CNY/m^3	2.71 CNY/m^3	9.7% lower
Platinum (Pt) Price	241.92 CNY/g	495 CNY/g	104.5% higher

Note: QE was not included in the break-even analysis because a ±10% variation in QE only resulted in a ±5.58% change in NPV (approximately ±0.68 million CNY), which is far less sensitive than the catalyst replacement interval, discount rate, or wastewater treatment fee. Influent COD concentration was also excluded from break-even calculations, as it represents an exogenous feedwater characteristic rather than a controllable project parameter; its impact is instead evaluated through scenario-based sensitivity analysis.

The sensitivity analysis reveals that both catalyst durability and feedwater consistency are critical determinants of economic viability. A reduction from 4.0 to 3.08 years is sufficient to drive the NPV to zero (Table 5), primarily due to the compounding cost of replacements and lost platinum recovery revenue. A tornado diagram (Figure 6) illustrates the relative influence of key techno-economic parameters on project NPV, thereby highlighting the catalyst replacement interval as the most sensitive factor. This parameter is directly threatened by irreversible Pt deactivation in the presence of industrial wastewater poisoning species such as sulfides, cyanides, or heavy metals (Section 2.1.1).

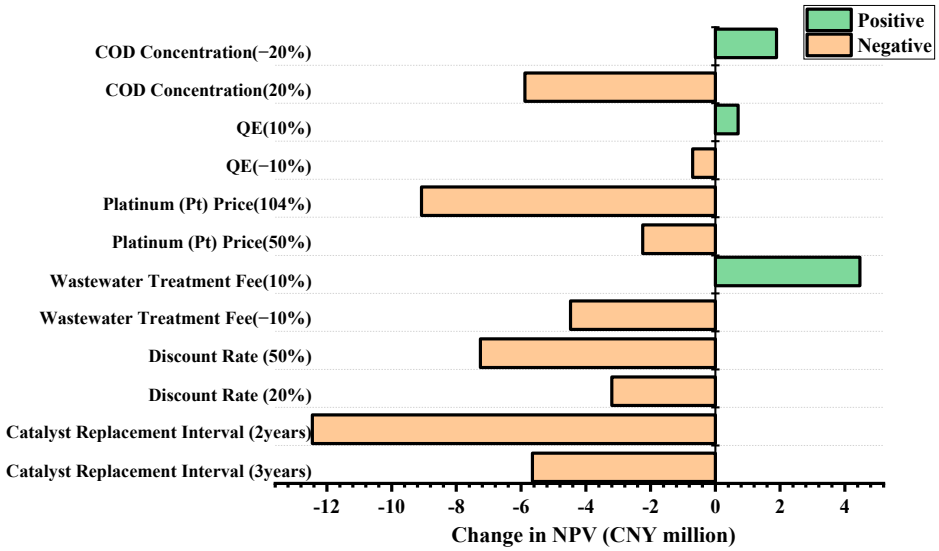


Figure 6. Tornado chart illustrating the relative influence of key techno-economic parameters on the project NPV.

Additionally, variations in COD concentration significantly affect the NPV. For instance, a 20% increase in influent COD concentration (to 360 mg/L), a plausible fluctuation in industrial effluents, reduces the NPV by 64.8% (from 9.08 to 3.20 million CNY).

In contrast, a ±10% variation in QE alters the NPV by only 7.7%, indicating that marginal gains in photocatalytic activity yield limited financial returns compared to improvements in operational stability or feedwater control. This insight shifts the R&D priority from purely activity-driven catalyst design to integrated strategies that enhance long-term robustness, such as optimizing Pt dispersion, surface passivation, or employing hybrid support matrices. These strategies aim to extend the operational life beyond the critical 3- to 4-year threshold. In parallel, this insight advocates for upstream wastewater equalization in cases where influent variability is high. Similarly, the impact of LED efficiency loss on NPV is relatively minor. Even under severe assumptions of post-replacement LED efficiency loss (down to 80% of the original), the NPV declines by less than 1% (from

9.08 to 8.99 million CNY). This indicates that the project's economics are highly resilient to moderate performance degradation in the light source, a common concern in long-term operation of photocatalytic systems. The limited impact stems from two factors: (1) The LED system accounts for only ~29% of total electricity demand; and (2) the degradation is confined to the final two years of the 10-year horizon, minimizing its discounted effect.

In stark contrast, the sensitivity of the project to the discount rate highlights a critical financing constraint. A modest increase in the discount rate from 10% to 12% reduces the NPV by 35.2% (Table 4), while the break-even analysis indicates that the maximum feasible discount rate is 15.9% (Figure 7). This narrow margin underscores the technology's dependence on access to low-cost capital, suggesting that economic viability is primarily achievable in contexts with preferential financing mechanisms such as green bonds, low-interest loans, or public–private partnerships. Given the high upfront CAPEX typical of advanced oxidation processes, this sensitivity reinforces the need for policy-driven financial de-risking to support early-stage deployment.

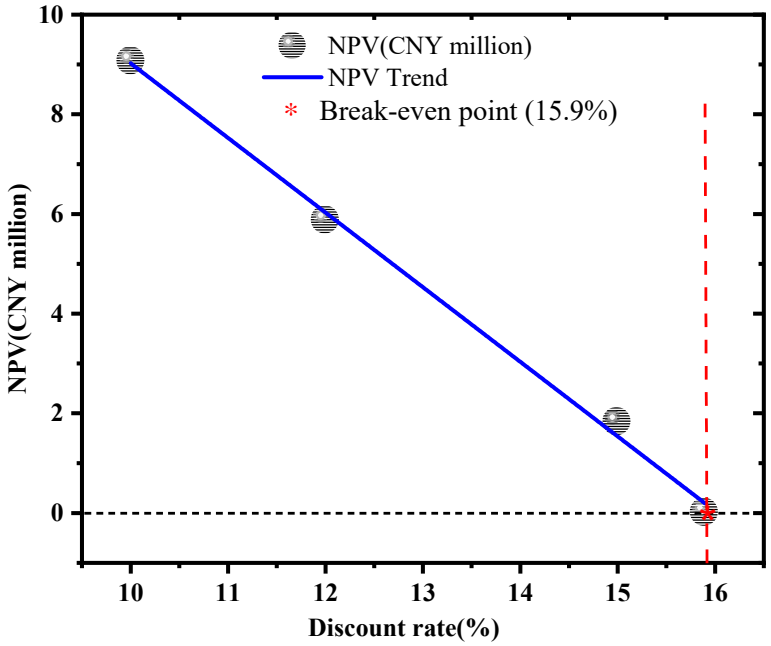


Figure 7. Variation in project NPV with discount rate, highlighting the break-even point at 15.9%.

Beyond financing conditions, revenue stability is equally pivotal. The wastewater treatment fee exhibits a near-linear relationship with NPV, with a 9.7% reduction (from 3.00 CNY/m^3 to 2.71 CNY/m^3) sufficient to drive the project to break-even (Table 5). This limited operational margin indicates low resilience to tariff fluctuations or competitive pricing pressures. Since treatment fees are often regulated or contractually negotiated with industrial clients, long-term revenue stability is essential for financial sustainability. The current fee of 3.00 CNY/m^3 implies that the technology is economically viable only when treating recalcitrant pollutants or meeting stringent effluent standards, positioning it for niche, high-value applications rather than bulk municipal wastewater treatment.

Compounding these financial vulnerabilities, input cost volatility—particularly in platinum—introduces further uncertainty. Although a 50% increase in platinum (Pt) price (to 362.85 CNY/g) results in a manageable decline in NPV to 6.84 million CNY, a 104.5% rise (to 495 CNY/g) eliminates all profitability (Tables 4 and 5). While this break-even threshold was estimated under historical price trends, recent market dynamics have seen Pt prices surge to approximately 387.56 CNY/g, representing a 60% increase over the base case. This development underscores the growing financial pressure on Pt-dependent technologies

and highlights the limitations of static cost assumptions in long-term techno-economic analysis. The partial recovery of Pt during catalyst replacement (1.56 million CNY per cycle) thus provides some mitigation but does not fully insulate the system from such volatility. Therefore, the current market trajectory reinforces the study's central conclusion: while the Pt/TiO_2 system may remain viable in the short term under favorable conditions, its long-term sustainability is increasingly contingent upon strategic risk mitigation, including supply chain diversification, investment in closed-loop Pt recycling, or a transition toward non-noble-metal alternatives.

In summary, the economic performance of the industrial-scale Pt/TiO_2 photocatalytic system is governed by three interdependent factors: catalyst durability, cost of capital, and market stability. Achieving scalable deployment will require not only technological innovation but also alignment with supportive policy frameworks, including R&D incentives, carbon pricing, and green financing mechanisms, to mitigate financial and market risks [49].

3.3. Strategic Directions for Technological Optimization

The sensitivity analysis in Section 3.2 reveals that the economic viability of the Pt/TiO_2 system, while positive under baseline conditions, is highly sensitive to several key parameters. To enhance the technology's financial resilience and broaden its applicability, we evaluate three alternative optimization pathways: non-metallic catalysts, hybrid process integration, and advanced reactor design.

It should be noted that our baseline techno-economic model assumes steady-state influent conditions to ensure analytical tractability. However, real-world applications often face significant feedwater variability. Recognizing this limitation, we explicitly address the economic and operational risks posed by COD fluctuations in this section and advocate for resilient design strategies, including hybrid process integration, modular reactor architectures, and, where feasible, upstream equalization, to buffer against such uncertainties.

Non-metallic photocatalysts such as graphitic carbon nitride ($g\text{-}C_3N_4$) reduce capital expenditure and life-cycle cost volatility by eliminating reliance on noble metals [50]. However, their lower QE and limited operational stability often counteract initial cost savings [51]. To achieve economic competitiveness with Pt/TiO_2 under current conditions, non-metallic catalysts must exhibit a service life exceeding 3.08 years, the break-even threshold identified in Section 3.2. Shorter replacement intervals result in frequent replacements and higher energy consumption, undermining cost advantages. Moreover, unlike Pt/TiO_2, these systems do not generate residual value from metal recovery, increasing the net replacement cost. Therefore, research should focus on enhancing long-term durability under realistic wastewater conditions, including resistance to fouling, photodegradation, chemical poisoning, and consistent performance across variable organic loads rather than short-term performance improvements under idealized laboratory settings [52].

While the economic potential of hybrid process integration (e.g., photocatalysis coupled with biological treatment) has been established in Section 2.2.3, its successful implementation faces significant engineering challenges. The primary hurdle lies in managing the increased system complexity, which introduces dual economic and operational risks. Economically, higher initial investment for additional reactors and advanced control systems can extend payback periods. Technically, fluctuations in the quality of photocatalytic effluent and the potential toxicity of reaction intermediates may destabilize downstream biological processes [42]. Importantly, hybrid configurations may also mitigate the economic impact of influent COD variability by leveraging the buffering capacity of biological units, thereby enhancing overall robustness of the system. Consequently, realizing the theoretical OPEX savings requires rigorous design, robust process control, and skilled operation [53].

Pilot-scale validation is therefore essential to quantify the true degree of process synergy, assess long-term stability, and confirm energy savings before full-scale deployment.

In addition to catalyst composition, reactor design significantly influences process efficiency and economic performance [54]. Advances in light distribution, modular scalability, and in situ catalyst management can improve photon utilization and extend maintenance intervals. For instance, enhanced irradiation uniformity may partially compensate for low QE, while modular reactor designs facilitate staged capacity expansion and simplified maintenance [55]. Such engineering improvements contribute to longer effective catalyst lifetimes and higher system reliability, directly addressing the high sensitivity of NPV to replacement frequency and energy demand under variable loading conditions observed in previous analysis.

In conclusion, although the Pt/TiO_2 system remains economically viable under favorable assumptions, increasing exposure to material and market risks underscores the strategic importance of alternative pathways. Non-metallic catalysts, hybrid processes, and advanced reactor designs each provide distinct opportunities to enhance cost resilience. Realizing their potential will require targeted advancements in durability, process integration, and system engineering, supported by policies that promote sustainable technological innovation.

4. Policy and Behavioral Interventions

4.1. Scope and Limitations

This study offers a strategic viewpoint on the industrialization of photocatalysis. However, it is important to recognize certain boundary conditions and inherent limitations.

The model is tailored for a specific scale (10,000 m^3/d) within the economic context of industrial China. Due to the significant economies of scale linked with AOPs, the findings may not be directly relevant to smaller-scale installations (<1000 m^3/d), where cost structures are impacted by varying levels of modularity and automation [56]. Additionally, the model outputs are influenced by region-specific factors, such as electricity pricing and the structure of carbon pricing mechanisms [57].

The analysis assumes a typical recalcitrant wastewater composition. In practical scenarios, catalyst performance and replacement could be affected by specific effluent components such as radical scavengers (e.g., carbonate, chloride), high salinity, and pH buffering capacity, which were not explicitly considered in the model. Therefore, site-specific pilot testing is crucial to validate the technical performance before full-scale implementation.

The techno-economic evaluation relies on current technological standards for photocatalysts and LED systems. However, advancements in non-noble-metal catalysts and high-efficiency light sources could significantly enhance cost-effectiveness. These innovations might expedite economic feasibility, thereby reducing both the projected payback period and the expected necessity for policy interventions.

The financial model utilizes a simplified depreciation schedule and does not consider intricate fiscal incentives beyond the standard corporate tax rate. The policy scenarios presented are illustrative, aiming to showcase potential mechanisms rather than provide precise recommendations for specific regulatory frameworks.

Future research should concentrate on validating the model with empirical data from long-term pilot operations [25]. Improving the framework by dynamically linking QE with reactor configuration, hydraulic retention time (HRT), and CAPEX would enhance its predictive capability. Additionally, applying the model across various industrial sectors and geographic regions is crucial for developing context-specific strategies to promote wider adoption of photocatalytic wastewater treatment.

4.2. Policy-Driven Mechanisms

The essence of successful policy formulation involves quantifying and internalizing environmental externalities to create dynamic incentive and constraint mechanisms [58]. One key approach is to develop a subsidy model that is dynamically linked to technological advancements and environmental advantages. This subsidy model can be expressed as

$$S = \alpha(C_b - C_a) + \beta \cdot E_C \quad (2)$$

where S is the subsidy amount per m^3 of treated water, C_a is the actual treatment cost per m^3, C_b is the economic feasibility threshold (i.e., the break-even cost determined by NPV = 0), and E_C quantifies the technology's carbon emission reduction contribution. The coefficients α and β reflect the technology's maturity level and the policy weight assigned to national carbon neutrality goals, respectively.

This model translates firms' cost-reduction efforts (as reflected in a decreasing C_a) and enhanced ecological performance (an increase in E_C) into stronger subsidy intensity, thereby creating incentives to continuously address key technical bottlenecks such as extending catalyst replacement interval. Financial instruments such as green credit can be utilized to provide low-interest loans and fast-tracked approval channels for manufacturers of photocatalytic equipment [59–61]. This approach alleviates heavy capital-expenditure pressures during the initial stages of large-scale production. Furthermore, promoting the inclusion of photocatalytic technology in national green-technology catalogs would enable its carbon-reduction benefits to be monetized through carbon credit trading markets [62,63].

The CO_2 emission reduction can be estimated by comparing the life-cycle greenhouse gas (GHG) emissions of photocatalytic treatment against a conventional baseline (e.g., activated sludge combined with chemical oxidation). While no specific carbon accounting methodology for photocatalytic wastewater treatment has yet been approved under major carbon markets (e.g., China's Certified Emission Reduction scheme [CCER] or the UNFCCC Clean Development Mechanism [CDM]), the quantification can be conceptually grounded in established LCA principles and existing wastewater-related emission factors from databases such as Ecoinvent or IPCC guidelines. Specifically, EC may be approximated as

$$EC = \left(EF_{conv} - EF_{photo}\right) \times Q \quad (3)$$

where EFconv and EFphoto represent the cradle-to-gate emission intensities (kg CO_2-eq/m^3) of the conventional and photocatalytic systems, respectively, and Q is the treated volume (m^3). Key contributors to emission differentials include (i) avoided methane emissions from reduced sludge generation, (ii) lower upstream emissions from eliminated or reduced chemical consumption, and (iii) decreased grid electricity use due to solar-driven operation.

Although such reductions cannot currently be directly monetized through formal carbon credit mechanisms, they represent verifiable co-benefits that could support future eligibility [64]. Policy efforts to expedite the approval of accounting methodologies for emerging water treatment technologies would thus be critical to unlock this revenue stream and strengthen the economic case for disruptive innovations like photocatalysis [65].

These measures can establish a positive feedback loop where technological improvement reduces costs, attracting greater subsidy support and financing access, thus fostering continued innovation and market diffusion [66].

4.3. Behavioral Economics Interventions

To lower adoption barriers for end users, intervention tools grounded in behavioral economics can be designed to manage risk perception and mitigate path dependence. First, establishing government-led technology demonstration zones can provide public testing

platforms and subsidies for first-of-a-kind (FOAK) equipment, enabling potential users to adopt the technology on a trial basis rather than assuming immediate full procurement responsibility [67]. This mechanism mitigates concerns about long-term stability by generating site-specific empirical evidence and enhances investment confidence through demonstration effects.

Second, a differentiated environmental taxation system can be implemented. Firms continuing to use high-pollution processes, such as the Fenton method, would be subject to a progressive environmental tax linked to pollutant toxicity and process carbon footprint, whereas adopters of cleaner technologies like photocatalysis would be eligible for tax credits or deductions [68,69]. This measure makes the implicit environmental costs of legacy technologies explicit, reshapes corporate cost–benefit calculations, and creates strong external pressure to upgrade [70].

Third, forming an industry-chain risk-sharing alliance is proposed. A consortium comprising catalyst suppliers, water utilities, and insurance institutions would establish a dedicated insurance fund for technology iteration and operational disruption [71]. This fund would collectively hedge operational risks arising from unforeseen catalyst failures or system malfunctions, thereby addressing end users' reluctance to adopt new technologies due to perceived operational risks [72].

5. Conclusions and Future Outlook

The industrialization of photocatalytic wastewater treatment presents a complex engineering challenge that requires optimizing environmental chemistry mechanisms and developing cost-effective models in tandem [73]. This study asserts that improving chemical efficiency can only lead to widespread industrial adoption by effectively managing life-cycle costs. Conversely, economic considerations can offer valuable insights for guiding technological research and development. In the context of industrializing photocatalytic wastewater treatment, the interaction between technology and economics is most evident at three key levels.

Catalyst carrier immobilization techniques and stabilization strategies for non-noble-metal active sites can prolong the material replacement interval and reduce dependence on noble metals [74,75]. These advancements offer direct economic benefits, enhancing the financial sustainability and risk resilience of projects [76]. System integration of photocatalysis with units like membrane separation, while increasing the initial investment, generates synergistic gains in energy consumption and anti-fouling through a degradation–separation approach. This results in marginal cost advantages that can be quantified using an LCA model and improves long-term operational stability. Furthermore, the substantial economic value of environmental and social benefits, such as reducing sludge volume, cutting carbon emissions [77], and mitigating public health risks [78], should be quantified through dynamic subsidies, carbon markets, and green financial instruments [79]. This is essential to offset the competitive disadvantage stemming from the cost premium associated with new technologies.

To overcome the industrialization bottlenecks in photocatalytic wastewater treatment, comprehensive innovation in chemistry, economics, and methodology is essential. In the chemical domain, improving catalytic performance by enhancing the separation efficiency of photogenerated charges through surface chemical modification and microstructural control is crucial [80,81]. Addressing challenges such as low QE and reliance on noble metals is necessary to advance material performance for practical applications [82]. Economically, establishing a multi-level environmental benefit accounting system that considers implicit benefits such as reduced health risks and long-term ecosystem restoration values is key [79,83]. Connecting carbon trading markets with water rights trading

mechanisms can create compensation pathways for positive externalities, encouraging green technology innovation [84,85]. Methodologically, developing an AI-driven, multi-scale R&D platform that integrates molecular-level catalyst performance prediction with engineering-level cost–benefit models can efficiently screen optimal solutions that meet technical and economic requirements, thus accelerating R&D efficiency and technology commercialization [86–88].

In the long term, photocatalytic technology should be deeply integrated with solar energy utilization and resource recovery pathways, forming a cost-recovery system that combines pollution control with energy production and helps evolve wastewater treatment units into hubs for resource generation and carbon reduction [89,90]. Under the synergistic effect of policy and digital transformation, this technology is poised to become a cost-effective solution for treating high-toxicity, recalcitrant industrial wastewater and serving regional carbon neutrality strategies [91–93]. Only when breakthroughs in chemical mechanisms and innovations in economic models form a verifiable, tradable, and replicable positive feedback loop can photocatalytic wastewater treatment technology cross the valley of death from laboratory to industrialization and mature into a key technology supporting sustainable development goals.

Author Contributions: Conceptualization, H.L. and M.S.; methodology, H.L.; software, H.L.; validation, H.L. and M.S.; formal analysis, H.L.; investigation, M.S.; resources, M.S.; data curation, H.L.; writing—original draft preparation, H.L.; writing—review and editing, H.L.; visualization, M.S.; supervision, M.S.; project administration, H.L.; funding acquisition, H.L. All authors have read and agreed to the published version of the manuscript.

Funding: This paper is funded by Philosophy and Social Science Research Projects of Jiangsu Universities (NO. 2021SJA0659); Philosophy and Social Science Research Projects of Nanjing University of Industry Technology (NO. 2021SKYJ11).

Data Availability Statement: The original contributions presented in this study are included in the article. Further inquiries can be directed to the corresponding author.

Conflicts of Interest: The authors declare no conflicts of interest.

Abbreviations

The following abbreviations are used in this manuscript:

Abbreviation	Full Name
A^2/O	Anaerobic–Anoxic–Oxic
CAPEX	Capital Expenditure
D&A	Depreciation and Amortization
EBT	Earnings Before Tax
MBBR	Moving Bed Biofilm Reactor
MBR	membrane bioreactor
NCF	Net Cash Flow
NPV	Net Present Value
OPEX	Operating Expenses
PBCM	Process-based cost model
QE	Quantum efficiency
TOU	Time of use

Appendix A

Appendix A.1. Operating Revenue

The project generates revenue solely from wastewater treatment service fees. The unit charge is set at 3.00 CNY per m^3, as stipulated by the Jiangsu Provincial Measures

for the Collection and Use of Wastewater Treatment Fees. This rate is consistent with the standard tariffs for industrial-scale treatment facilities in the region and reflects a balance between cost recovery and regulatory affordability. With a design capacity of 10,000 m^3/d and assuming full utilization, the annual operating revenue is estimated at 10.95 million CNY.

Appendix A.2. Operating Costs

Appendix A.2.1. Annual Electricity Cost for the Project

Photocatalytic processes are inherently limited by low QE, necessitating high-power irradiation to achieve target pollutant removal rates at scale. To address this, the system employs a UVA-LED array (365 nm) selected for its energy efficiency and operational durability. The total installed electrical load is 280 kW, comprising 80 kW for the photocatalytic unit and 200 kW for auxiliary systems (pumps, blowers, and control systems). This power allocation is consistent with energy profiles observed in comparable A^2/O-MBR installations [94], adjusted for the enhanced photon utilization of the proposed reactor design.

Electricity costs were calculated using the latest time-of-use (TOU) tariff structure for industrial users, as stipulated in Document No. [2025] 426 issued by the Jiangsu Provincial Development and Reform Commission. The facility operates under a two-part tariff (energy + capacity charges) at the 1–10 kV voltage level, with a contracted capacity of 400 kVA. The base electricity price during the flat period was calculated as 0.5497 CNY/kWh, comprising the grid access charge (0.3910 CNY/kWh), transmission and distribution fee (0.1357 CNY/kWh), and additional surcharges (0.0230 CNY/kWh). Time-of-use tariffs were applied according to seasonal operational profiles: during summer and winter (181 days), the daily load was distributed across critical peak (3 h), peak (5 h), flat (8 h), and off-peak (8 h) periods; during spring and autumn (184 days), the distribution was peak (7 h), flat (8 h), and off-peak (9 h). Based on continuous operation at 280 kW, the annual energy charge amounted to 1.4045 million CNY, with an additional 0.1536 million CNY in capacity charges (400 kVA × 32 CNY/kVA/month × 12 months), yielding a total annual electricity cost of 1.5581 million CNY, equivalent to an effective average electricity rate of 0.636 CNY/kWh (Calculation steps are summarized in Tables A1–A4).

Table A1. Determination of Base Tariff and Price Fluctuation Ratios.

Parameter	Basis/Source	Value/Result
Voltage level	Project design assumption	1–10 kV
Billing mechanism	Determined by project scale	Two-part tariff
Transmission and distribution price	Jiangsu Grid Transmission and Distribution Price Table, 1–10 kV two-part tariff	0.1357 CNY/kWh
Grid-connected electricity price	Benchmark coal-fired power price in Jiangsu Province	0.3910 CNY/kWh
Additional surcharge	Capacity cost allocation for natural gas power generation	0.0230 CNY/kWh
Base price (Flat period)	Sum: Transmission + Grid-connected + Surcharge	0.5497 CNY/kWh
Peak/Off-peak fluctuation ratio	Two-part tariff system	Peak: 80%; Off-peak: −65%
Critical peak/Deep off-peak ratio	Applicable to industrial loads >315 kVA	Critical peak: 20% above peak price

Notes: All prices are in CNY. The two-part tariff system includes both energy-based (kWh) and capacity-based (kVA) charges. The critical peak pricing applies to industrial users with contracted capacity exceeding 315 kVA.

Table A2. Calculation of Final Electricity Tariffs by Period.

Time-of-Use Period	Calculation Formula	Final Price (CNY/kWh)
Flat period	0.5497 (base)	0.5497
Off-peak period	0.5497 × (1 − 65%)	0.1924
Peak period	0.5497 × (1 + 80%)	0.9895
Critical peak period	0.9895 × (1 + 20%)	1.1874

Table A3. Seasonal and Time-of-Use-Based Annual Energy Charge Calculation.

Season	Time Period	Daily Duration (h)	Days	Energy Charge Formula (CNY)	Total Energy Charge (Million CNY)
Summer/Winter	Critical peak	3	181	3 h × 181 d × 280 kW × 1.1874 CNY/kWh	0.18
	Peak	5	181	5 h × 181 d × 280 kW × 0.9895 CNY/kWh	0.25
	Flat	8	181	8 h × 181 d × 280 kW × 0.5497 CNY/kWh	0.22
	Off-peak	8	181	8 h × 181 d × 280 kW × 0.1924 CNY/kWh	0.08
Spring/Autumn	Peak	7	184	7 h × 184 d × 280 kW × 0.9895 CNY/kWh	0.36
	Flat	8	184	8 h × 184 d × 280 kW × 0.5497 CNY/kWh	0.23
	Off-peak	9	184	9 h × 184 d × 280 kW × 0.1924 CNY/kWh	0.09
Total			365	Sum of all periods charges	1.41

Notes: The year is divided into two seasonal regimes: summer/winter (181 days) and spring/autumn (184 days).

Table A4. Calculation of Total Annual Electricity Cost.

Cost Category	Basis/Formula	Annual Cost (Million CNY)
Annual energy charge	From Table A3	1.41
Annual capacity charge	400 kVA × 32.0 CNY/month × 12 months	0.15
Total annual electricity cost	Energy + Capacity charge	1.56
Equivalent average electricity price	1.56 million CNY/(280 × 24 × 365) kWh	0.636 CNY/kWh

Notes: The total annual electricity cost comprises two components: energy charge and capacity charge.

Appendix A.2.2. Labor and Maintenance Costs

Annual labor costs are budgeted at 0.48 million CNY for a team of four. Annual maintenance costs are set at 0.30 million CNY, covering both conventional equipment (e.g., pumps and blowers) and the specialized photocatalytic system. The former is estimated at approximately 0.24 million CNY, derived from a 3% annual maintenance rate applied to the 8 million CNY investment in conventional equipment. The latter, which includes periodic LED cleaning, control system inspections, and sensor calibration, involves low labor intensity and is projected at 0.06 million CNY.

Appendix A.3. Investment

Appendix A.3.1. Supporting Carrier

For a 10,000 m^3/d water treatment plant, a high specific surface area (>500 m^2/m^3) is essential to ensure sufficient contact time and reaction efficiency. A carrier volume of 500 m^3 aligns with typical HRT (e.g., 1–1.5 h) in industrial-scale systems. The unit price of CNY 1200/m^3 represents a moderate-to-low estimate within the industrial market range (typically CNY 1000–2500/m^3), reflecting cost-effective, commercially available

honeycomb ceramics or structured packing materials with adequate mechanical strength and porosity [95]. Therefore, the total carrier cost is estimated at 6 million CNY.

Appendix A.3.2. UVA-LED Light Sources

Industrial UVA-LED modules (365–385 nm), including drivers, liquid cooling, and optics, are estimated to cost 8 million CNY for 80 kW of installed power (CNY 100/W). This conservative unit cost accounts for industrial-grade components, thermal management, and long-term reliability under continuous operation. Notably, this power demand is lower than that of conventional UV-AOP systems, which typically require 100–200 kW for comparable treatment capacity [96]. The reduction stems from the high QE of the tailored photocatalyst and optimized reactor geometry, enhancing photon utilization and yielding lower Lighting CAPEX and operational energy costs.

Appendix A.3.3. Catalyst

The catalyst loading of 730 kg (1.75 kg/m^3) is based on a design approach informed by pilot-scale immobilized TiO_2 systems, which have demonstrated effective pharmaceutical removal and scalability for real-world wastewater treatment applications [97,98]. The catalyst is platinum-based with a Pt loading of 1 wt%. Based on the platinum market price of CNY 241.92/g (source: Shanghai Gold Exchange), the raw material cost for the initial charge is calculated to be approximately 1.77 million CNY. Accounting for synthesis, immobilization, quality control, and engineering overheads, the total project cost is estimated as 2.5 times the raw material cost, leading to an initial engineering market quotation of 4.43 million CNY for the catalyst system [99].

A catalyst replacement interval of 4 years is adopted as a conservative baseline for the immobilized Pt/TiO_2 system. This estimate is consistent with engineering extrapolations from long-term solar photocatalytic trials, which demonstrate sustained activity of TiO_2-based photocatalysts over hundreds of hours [99]. For instance, pilot-scale compound parabolic collector studies have reported negligible deactivation after several hundred hours of continuous solar treatment of organic pollutants under natural sunlight [100], while a solar-driven disinfection study using immobilized TiO_2 showed only a ~0.5 percentage-point decline in bacterial inactivation efficiency (from 99.9% to 99.4%) after 250 h of operation [101]. Although these references focus on unmodified TiO_2, the incorporation of Pt is well documented to improve charge separation and mitigate photocorrosion, suggesting that Pt/TiO_2 systems may achieve comparable or superior stability under analogous operating conditions [102,103].

Critically, the catalyst's service life depends on both periodic maintenance (e.g., rinsing to mitigate fouling) and the quality of pre-treated feedwater, specifically its content of sulfides, heavy metals, and suspended solids [104]. Therefore, to reflect this uncertainty, a sensitivity analysis considering catalyst lifetimes between 2 and 6 years is provided in Section 3.3.

Appendix A.3.4. Reactor System

The reactor structure, including the vessel, internal flow distributors, supports, and integration components, is estimated at 8 million CNY. This estimate follows established cost correlations for large-scale chemical process equipment [105], adjusted for the use of stainless steel and custom fabrication.

Appendix A.3.5. Working Capital Reserve

A working capital reserve of 4 million CNY is included to ensure operational continuity during commissioning, maintenance, and supply chain disruptions. This amount

represents approximately 15% of the total fixed capital investment, within the typical range (10–15%) for industrial process facilities [106]. Given the reliance on high-value catalysts and scheduled replacements, a slightly higher allocation is justified.

Appendix A.3.6. Depreciation and Amortization (D&A)

Straight-line depreciation is applied to all capitalized components over service lives consistent with engineering and operational expectations [107]: 8 years for UVA-LED systems, 4 years for the photocatalyst, and 10 years for the reactor and carrier support. These replacement intervals follow typical design and replacement cycles reported for photocatalytic and UV-AOP systems [95]. A 10% salvage value is assigned exclusively to the reactor–carrier system, reflecting its longer durability and residual material value [107]. The resulting annual D&A charge amounts to 3.37 million CNY. Major reinvestments, specifically catalyst replacement in Year 4 and LED module renewal in Year 8, are modeled as discrete cash outflows, with platinum recovery from spent catalysts treated as a concurrent cash inflow. This approach ensures stable D&A for financial reporting while accurately capturing the timing of major expenditures in the cash flow analysis.

Appendix A.4. Discount Rate

A 10% discount rate is consistent with the weighted average cost of capital estimates for emerging low-carbon technologies under moderate risk assumptions [108]. While higher rates (e.g., 12–15%) may apply under elevated risk perceptions, this base-case value reflects a balanced assessment of technological maturity and financing conditions for demonstration-scale deployments.

Table A5. Base-Case Parameters and Sources.

Category	Parameter	Base Value	Unit	Basis/Source
Capacity	Design throughput	10,000	m^3/d	Project design specification
Horizon	Project lifetime	10	years	Base case
Financial	Discount rate	10%	—	(Appendix A.4) [108]
Electricity	TOU blended tariff	0.636	CNY/kWh	(Appendix A.2.1) Jiangsu Provincial Measures for the Collection and Use of Wastewater Treatment Fees
OPEX	Annual Electricity Cost	1.56	million CNY	
OPEX	Labor costs	0.48	million CNY	(Appendix A.2.2)
OPEX	Maintenance Cost	0.30	million CNY	
OPEX	Annual base OPEX	2.34	million CNY	
CAPEX	Reactor System Cost	8.00	million CNY	(Appendix A.3.4) [105]
CAPEX	UVA-LED Light Sources	8.00	million CNY	(Appendix A.3.2) [96]
CAPEX	Carrier Support	6	million CNY	(Appendix A.3.1) [95]
CAPEX	Catalyst system	4.43	million CNY	(Appendix A.3.3) [99]
CAPEX	Working Capital Reserve	4	million CNY	(Appendix A.3.3) [106]
CAPEX	Total initial CAPEX	30.43	million CNY	Project budget
Depreciation	Method	Straight-line	—	Accounting policy
Depreciation	Reactor System	10	years	(Appendix A.3.6) [99,107]
Depreciation	LED	8	years	
Depreciation	Catalyst	4	years	

Table A5. *Cont.*

Category	Parameter	Base Value	Unit	Basis/Source
Depreciation	Annual Depreciation And Amortization (D&A)	3.37	million CNY	
Salvage	Reactor + Carrier	10%	of initial CAPEX	
Platinum	Initial Pt mass	7.30	kg	Based on 730 kg catalyst bed with 1% Pt loading (Appendix A.3.3) [82,83]
Platinum	Pt market price	241.92	CNY/g	The average of the end-of-month closing prices from the Shanghai Gold Exchange over the past three years (Appendix A.3.3)
Platinum	Physical recovery rate	98%	—	
Platinum	Service fee rate	10%	—	Appendix B [109]
Terminal	Net Pt recovery	1.56	million CNY	

Note: The parameters detailed above form the basis for subsequent sensitivity and scenario analyses, with a particular focus on the catalyst replacement interval, discount rate, wastewater treatment fee, and platinum price volatility. These are identified as key drivers of project economics.

Appendix B

Platinum recovery constitutes the primary economic benefit of catalyst recycling. An overall platinum recovery rate of 98% is assumed, which is well supported by experimental studies reporting platinum leaching efficiencies of up to 98.1% under optimized mild leaching conditions [109]. When coupled with efficient downstream refining processes, such high leaching performance enables near-complete metal recovery. Furthermore, a service fee of 10% of the recovered platinum's market value is consistent with industry practice, commonly applied in third-party precious metal recycling agreements to cover processing, logistics, and operational overhead costs.

Table A6. Calculation of Net Platinum Recovery Revenue from Spent Catalyst.

Description	Symbol	Value/Formula	Result (Million CNY)
Input Parameters			
Initial Platinum Mass	$M_{Pt,initial}$	7.30 kg	—
Platinum Market Price	P_{Pt}	241.92 CNY/g	—
Physical Recovery Rate	$\eta_{physical}$	98%	—
Service Fee Rate	$f_{service}$	10%	—
Calculation			
Gross Market Value	V_{gross}	$M_{Pt,initial} \times \eta_{physical} \times PPt$	1.73
Service Charge	$C_{service}$	$V_{gross} \times f_{service}$	0.17
Net Recovery Revenue	$R_{net,recovery}$	V_{gross}-$C_{service}$	1.56

Appendix C

Table A7. Comparison of Methodological Features Between Conventional LCA/LCCA approaches and the Proposed Dynamic NPV Framework.

Feature	Typical LCA/LCCA Studies	This Study's Dynamic NPV Framework
Time resolution	Static or annual average	Annual cash flows with explicit replacement years (Y4, Y8)
Catalyst cost treatment	Fixed OPEX or lumped CAPEX	Dynamic replacement + Pt recovery credit

Table A7. *Cont.*

Feature	Typical LCA/LCCA Studies	This Study's Dynamic NPV Framework
Technical constraints	Frequently simplified or assumed within nominal operating ranges	Explicitly bounded by COD, turbidity, poison limits (Section 2.1.1)
Revenue stream	Rarely included	Treatment fee + Pt salvage value
Decision output	Environmental impact/total cost	NPV, break-even thresholds, sensitivity rankings

References

1. Saravanan, A.; Senthil Kumar, P.; Jeevanantham, S.; Karishma, S.; Tajsabreen, B.; Yaashikaa, P.R.; Reshma, B. Effective Water/Wastewater Treatment Methodologies for Toxic Pollutants Removal: Processes and Applications towards Sustainable Development. *Chemosphere* **2021**, *280*, 130595. [CrossRef]
2. Cui, Z.; Yuan, R.; Chen, H.; Zhou, B.; Zhu, B.; Zhang, C. Application of Polyaniline-Based Photocatalyst in Photocatalytic Degradation of Micropollutants in Water: A Review. *J. Water Process Eng.* **2024**, *59*, 104900. [CrossRef]
3. Yeneneh, A.M.; Al Balushi, K.; Jafary, T.; Al Marshudi, A.S. Hydrodynamic Cavitation and Advanced Oxidation for Enhanced Degradation of Persistent Organic Pollutants: A Review. *Sustainability* **2024**, *16*, 4601. [CrossRef]
4. Luo, B.; He, H.; Yan, Y.; Wang, Y.; Yang, X.; Liu, Y.; Xu, J.; Huang, W. Flocculants for the High-Concentration Activated Sludge Method and the Effectiveness of Urban Wastewater Treatment. *Water* **2024**, *16*, 2281. [CrossRef]
5. Ferrentino, R.; Langone, M.; Fiori, L.; Andreottola, G. Full-Scale Sewage Sludge Reduction Technologies: A Review with a Focus on Energy Consumption. *Water* **2023**, *15*, 615. [CrossRef]
6. Yu, P.; Tu, W.; Wu, M.; Zhang, Z.; Wang, H. Pilot-Scale Fermentation of Urban Food Waste for Volatile Fatty Acids Production: The Importance of pH. *Bioresour. Technol.* **2021**, *332*, 125116. [CrossRef] [PubMed]
7. Zieliński, M.; Kazimierowicz, J.; Dębowski, M. Advantages and Limitations of Anaerobic Wastewater Treatment—Technological Basics, Development Directions, and Technological Innovations. *Energies* **2022**, *16*, 83. [CrossRef]
8. Jiang, L.; Yang, J.; Zhou, S.; Yu, H.; Liang, J.; Chu, W.; Li, H.; Wang, H.; Wu, Z.; Yuan, X. Strategies to Extend Near-Infrared Light Harvest of Polymer Carbon Nitride Photocatalysts. *Coord. Chem. Rev.* **2021**, *439*, 213947. [CrossRef]
9. Loeb, S.K.; Alvarez, P.J.J.; Brame, J.A.; Cates, E.L.; Choi, W.; Crittenden, J.; Dionysiou, D.D.; Li, Q.; Li-Puma, G.; Quan, X.; et al. The Technology Horizon for Photocatalytic Water Treatment: Sunrise or Sunset? *Environ. Sci. Technol.* **2019**, *53*, 2937–2947. [CrossRef]
10. Zhao, S.-Z.; Lu, Y.; Lu, R.; Hu, Y.-D.; Rodriguez, R.D.; Chen, J.-J. Constructing BiOBr/TiO_2 Heterostructure Nanotubes for Enhanced Adsorption/Photocatalytic Performance. *J. Water Process Eng.* **2023**, *54*, 103972. [CrossRef]
11. Yang, J.; Wang, H.; Jiang, L.; Yu, H.; Zhao, Y.; Chen, H.; Yuan, X.; Liang, J.; Li, H.; Wu, Z. Defective Polymeric Carbon Nitride: Fabrications, Photocatalytic Applications and Perspectives. *Chem. Eng. J.* **2022**, *427*, 130991. [CrossRef]
12. Wu, H.; Li, L.; Wang, S.; Zhu, N.; Li, Z.; Zhao, L.; Wang, Y. Recent Advances of Semiconductor Photocatalysis for Water Pollutant Treatment: Mechanisms, Materials and Applications. *Phys. Chem. Chem. Phys.* **2023**, *25*, 25899–25924. [CrossRef]
13. Liu, W.; He, C.; Zhu, B.; Zhu, E.; Zhang, Y.; Chen, Y.; Li, J.; Zhu, Y. Progress in Wastewater Treatment via Organic Supramolecular Photocatalysts under Sunlight Irradiation. *Chin. J. Catal.* **2023**, *53*, 13–30. [CrossRef]
14. Ahtasham Iqbal, M.; Akram, S.; Khalid, S.; Lal, B.; Hassan, S.U.; Ashraf, R.; Kezembayeva, G.; Mushtaq, M.; Chinibayeva, N.; Hosseini-Bandegharaei, A. Advanced Photocatalysis as a Viable and Sustainable Wastewater Treatment Process: A Comprehensive Review. *Environ. Res.* **2024**, *253*, 118947. [CrossRef]
15. Mishra, S.; Sundaram, B. A Review of the Photocatalysis Process Used for Wastewater Treatment. *Mater. Today Proc.* **2024**, *102*, 393–409. [CrossRef]
16. Hassaan, M.A.; El-Nemr, M.A.; Elkatory, M.R.; Ragab, S.; Niculescu, V.-C.; El Nemr, A. Principles of Photocatalysts and Their Different Applications: A Review. *Top. Curr. Chem.* **2023**, *381*, 31. [CrossRef]
17. Rafieenia, R.; Sulonen, M.; Mahmoud, M.; El-Gohary, F.; Rossa, C.A. Integration of Microbial Electrochemical Systems and Photocatalysis for Sustainable Treatment of Organic Recalcitrant Wastewaters: Main Mechanisms, Recent Advances, and Present Prospects. *Sci. Total Environ.* **2022**, *824*, 153923. [CrossRef] [PubMed]
18. Paiu, M.; Lutic, D.; Favier, L.; Gavrilescu, M. Heterogeneous Photocatalysis for Advanced Water Treatment: Materials, Mechanisms, Reactor Configurations, and Emerging Applications. *Appl. Sci.* **2025**, *15*, 5681. [CrossRef]
19. Zheng, M.-W.; Tran, N.T.T.; Liu, S.-H. Enhanced Dual-Functional Performance on the Tetracycline Degradation and Chromium Detoxification via Z-Scheme COF/TiO_2-NH_2 Heterojunctions. *J. Water Process Eng.* **2025**, *78*, 108770. [CrossRef]
20. Duraimurugan, J.; Kumar, G.S.; Shanavas, S.; Ramesh, R.; Acevedo, R.; Anbarasan, P.M.; Maadeswaran, P. Hydrothermal Assisted Phytofabrication of Zinc Oxide Nanoparticles with Different Nanoscale Characteristics for the Photocatlytic Degradation of Rhodamine B. *Optik* **2020**, *202*, 163607. [CrossRef]

21. Gupta, B.; Saidulu, D.; Srivastava, A.; Rawat, A.; Singh, A.; Bhatnagar, A.; Gupta, A.K. Performance Assessment of Photo-Controlled Catalytic and Moving Biocarrier-Based Hybrid Systems for the Treatment of Pharmaceuticals from Municipal and Industrial Wastewater: Insights into Influencing Factors and Degradation Mechanisms. *J. Environ. Chem. Eng.* **2023**, *11*, 110128. [CrossRef]
22. Han, C.; Wang, Z.; Cui, J.; Liu, S.; Yang, L.; Fu, Y.; Zhu, B.; Guo, C. Rapid Quantitative Detection of Dye Concentration in Pt/TiO_2 Photocatalytic System Based on RGB Sensing. *Sensors* **2025**, *25*, 3195. [CrossRef]
23. Meena, P.L.; Poswal, K.; Surela, A.K.; Saini, J.K. Synthesis of G-C_3N_4/ZnO Nanostructures via Mechano-Thermal Method for Photocatalytic Degradation of Methylene Blue Dye. *Int. J. Environ. Sci. Technol.* **2025**, *22*, 833–848. [CrossRef]
24. Al Qaydi, M.; Rajput, N.S.; Lejeune, M.; Bouchalkha, A.; El Marssi, M.; Cordette, S.; Kasmi, C.; Jouiad, M. Intermixing of MoS_2 and WS_2 Photocatalysts toward Methylene Blue Photodegradation. *Beilstein J. Nanotechnol.* **2024**, *15*, 817–829. [CrossRef] [PubMed]
25. Iervolino, G.; Zammit, I.; Vaiano, V.; Rizzo, L. Limitations and Prospects for Wastewater Treatment by UV and Visible-Light-Active Heterogeneous Photocatalysis: A Critical Review. In *Heterogeneous Photocatalysis*; Muñoz-Batista, M.J., Navarrete Muñoz, A., Luque, R., Eds.; Topics in Current Chemistry Collections; Springer International Publishing: Cham, Switzerland, 2020; pp. 225–264, ISBN 978-3-030-49491-9.
26. Wang, L.; Zhang, Q.; Chen, B.; Bu, Y.; Chen, Y.; Ma, J.; Rosario-Ortiz, F.L.; Zhu, R. Some Issues Limiting Photo(Cata)Lysis Application in Water Pollutant Control: A Critical Review from Chemistry Perspectives. *Water Res.* **2020**, *174*, 115605. [CrossRef]
27. Qudsieh, I.Y.; Ali, M.A.; Maafa, I.M. Effect of Water Matrix on Photocatalytic Degradation of Organic Pollutants in Water: A Literature Review. *Rev. Chem. Eng.* **2025**, *41*, 539–573. [CrossRef]
28. Tawfik, A.; Alalm, M.G.; Awad, H.M.; Islam, M.; Qyyum, M.A.; Al-Muhtaseb, A.H.; Osman, A.I.; Lee, M. Solar Photo-Oxidation of Recalcitrant Industrial Wastewater: A Review. *Environ. Chem. Lett.* **2022**, *20*, 1839–1862. [CrossRef]
29. Donga, C.; Ratshiedana, R.; Kuvarega, A.T.; Masunga, N.; Vallabhapurapu, V.S.; Mbule, P. Photocatalytic Degradation of Organic Pollutants in Wastewater Using Magnetic Functionalized Reduced Graphene Oxide Nanocomposites. A Review. *Talanta* **2025**, *295*, 128318. [CrossRef]
30. Montenegro, R.; González, Z.; Rodríguez, A.; Canovi, C.; Pozzi, P.; Siligardi, C.; Cedillo-González, E.I. Processing of Bio-Based Photocatalytic Sponge-like Structures Containing C,N-TiO_2 Colloidally Dispersed onto Cellulose Nanofibers for Microplastic Remediation. *J. Environ. Manag.* **2025**, *389*, 126015. [CrossRef]
31. Díez, A.M.; Pazos, M.; Sanromán, M.Á.; Naranjo, H.V.; Mayer, J.; Kolen'ko, Y.V. Photocatalytic Solid-Phase Degradation of Polyethylene with Fluoride-Doped Titania under Low Consumption Ultraviolet Radiation. *J. Environ. Manag.* **2023**, *329*, 117044. [CrossRef]
32. Li, D.; Calebe, V.C.; Li, Y.; Liu, H.; Lei, Y. Interstitial N-Doped TiO_2 for Photocatalytic Methylene Blue Degradation under Visible Light Irradiation. *Catalysts* **2024**, *14*, 681. [CrossRef]
33. Yang, X.; Liang, J.; Fu, H.; Ran, X.; An, X. Fabrication of Au-Ag@TiO_2 Ternary Core-Shell Nanostructures with Enhanced Sunlight Photocatalytic Activity. *Powder Technol.* **2022**, *404*, 117463. [CrossRef]
34. Mei, X.; Yuan, H.; Li, C. Study on the MOF Frame Pt-TiO_2 Hybrid Photocatalyst and Its Photocatalytic Performance. *Sustainability* **2023**, *15*, 1403. [CrossRef]
35. Liu, J.; Zheng, J.; Yue, G.; Li, H.; Liu, Z.; Zhao, Y.; Wang, N.; Sun, C.; Cui, Z. Continuous G-C_3N_4 Layer-Coated Porous TiO_2 Fibers with Enhanced Photocatalytic Activity toward H_2 Evolution and Dye Degradation. *RSC Adv.* **2022**, *12*, 10258–10266. [CrossRef] [PubMed]
36. Chi, N.; Xu, W. Synthesis of TiO_2/g-C_3N_4 Hybrid Photocatalyst and Its Application for Degradation of Chlorophenol as Organic Water Pollutant. *Int. J. Electrochem. Sci.* **2022**, *17*, 220929. [CrossRef]
37. Lu, X.; Zhu, M.; Chen, D.; Wu, J.; Gao, S.; Zhao, Y.; Yang, J.; Li, S.; Meng, J. Preparation, Modification, and Application of Graphitic Carbon Nitride in Photocatalytic Degradation of Antibiotics. *Processes* **2025**, *13*, 3365. [CrossRef]
38. Yang, Y.; Wang, D.Y.; Zhang, Y.C.; Chen, S.Y.; Sun, Y. Enhanced Photocatalytic Performance of Z-Scheme TiO_2/g-C_3N_4 Heterojunction towards Degradation of Rhodamine B. *DJNB* **2022**, *17*, 1491–1500. [CrossRef]
39. Liu, Q.; Hou, J.; Zeng, Y.; Xia, J.; Miao, L.; Wu, J. Integrated Photocatalysis and Moving Bed Biofilm Reactor (MBBR) for Treating Conventional and Emerging Organic Pollutants from Synthetic Wastewater: Performances and Microbial Community Responses. *Bioresour. Technol.* **2023**, *370*, 128530. [CrossRef]
40. Chen, C.-Y.; Wang, G.-H.; Chang, Y.-J.; Chen, Y.-H.; Cheng, C.-Y.; Chung, Y.-C. Combination of a Highly Efficient Biological System and Visible-Light Photocatalysis Pretreatment System for the Removal of Phthalate Esters from Wastewater. *Water* **2022**, *14*, 3139. [CrossRef]
41. Liu, K.; Chen, J.; Sun, F.; Liu, Y.; Tang, M.; Yang, Y. Historical Development and Prospect of Intimately Coupling Photocatalysis and Biological Technology for Pollutant Treatment in Sewage: A Review. *Sci. Total Environ.* **2022**, *835*, 155482. [CrossRef]
42. Zhang, C.; Li, Y.; Shen, H.; Shuai, D. Simultaneous Coupling of Photocatalytic and Biological Processes: A Promising Synergistic Alternative for Enhancing Decontamination of Recalcitrant Compounds in Water. *Chem. Eng. J.* **2021**, *403*, 126365. [CrossRef]

43. López, J.L.C.; Reina, A.C.; Gómez, E.O.; Martín, M.M.B.; Rodríguez, S.M.; Pérez, J.A.S. Integration of Solar Photocatalysis and Membrane Bioreactor for Pesticides Degradation. *Sep. Sci. Technol.* **2010**, *45*, 1571–1578. [CrossRef]
44. Lu, Z.; Xu, Y.; Akbari, M.Z.; Liang, C.; Peng, L. Insight into Integration of Photocatalytic and Microbial Wastewater Treatment Technologies for Recalcitrant Organic Pollutants: From Sequential to Simultaneous Reactions. *Chemosphere* **2022**, *295*, 133952. [CrossRef]
45. De Abreu, V.H.S.; Pereira, V.G.F.; Proença, L.F.C.; Toniolo, F.S.; Santos, A.S. A Systematic Study on Techno-Economic Evaluation of Hydrogen Production. *Energies* **2023**, *16*, 6542. [CrossRef]
46. Esrafili, A.; Salimi, M.; Jonidi Jafari, A.; Reza Sobhi, H.; Gholami, M.; Rezaei Kalantary, R. Pt-Based TiO_2 Photocatalytic Systems: A Systematic Review. *J. Mol. Liq.* **2022**, *352*, 118685. [CrossRef]
47. Maurya, J.; Gemechu, E.; Kumar, A. The Development of Techno-Economic Assessment Models for Hydrogen Production via Photocatalytic Water Splitting. *Energy Convers. Manag.* **2023**, *279*, 116750. [CrossRef]
48. *GB 18918-2002*; Discharge Standard of Pollutants for Municipal Wastewater Treatment Plant. State Environmental Protection Administration: Beijing, China, 2002.
49. Antonietti, M.; Pelicano, C.M. Translating Laboratory Success into the Large-Scale Implementation of Photocatalytic Overall Water Splitting. *Front. Sci.* **2024**, *2*, 1507745. [CrossRef]
50. Ong, W.-J.; Tan, L.-L.; Ng, Y.H.; Yong, S.-T.; Chai, S.-P. Graphitic Carbon Nitride (g-C_3N_4)-Based Photocatalysts for Artificial Photosynthesis and Environmental Remediation: Are We a Step Closer To Achieving Sustainability? *Chem. Rev.* **2016**, *116*, 7159–7329. [CrossRef]
51. Singh, R.; Chauhan, M.; Garg, P.; Sharma, B.; Attri, P.; Sharma, R.K.; Sharma, D.; Chaudhary, G.R. A Critical Review on Visible Light Active Graphitic Carbon Nitride (g-CN) Based Photocatalyst for Environment Remediation Application: A Sustainable Approach. *J. Clean. Prod.* **2023**, *427*, 138855. [CrossRef]
52. Wang, Y.-D.; Lee, T.-W.; Lo, Y.-C.; Hong, W.-J.; Chen, C. Insights into Photochemical Stability of Graphitic Carbon Nitride-Based Photocatalysts in Water Treatment. *Carbon* **2021**, *175*, 223–232. [CrossRef]
53. Nidheesh, P.V.; Couras, C.; Karim, A.V.; Nadais, H. A Review of Integrated Advanced Oxidation Processes and Biological Processes for Organic Pollutant Removal. *Chem. Eng. Commun.* **2022**, *209*, 390–432. [CrossRef]
54. Toe, C.Y.; Pan, J.; Scott, J.; Amal, R. Identifying Key Design Criteria for Large-Scale Photocatalytic Hydrogen Generation from Engineering and Economic Perspectives. *ACS ES&T Eng.* **2022**, *2*, 1130–1143. [CrossRef]
55. Li, Y.; Zhang, D.; Ye, J.; Mai, Y.; Wang, C.; Yang, Y.; Li, Y.; Besenbacher, F.; Niemantsverdriet, H.; Rosei, F.; et al. A Modular Tubular Flow System with Replaceable Photocatalyst Membranes for Scalable Coupling and Hydrogenation. *Angew. Chem.* **2023**, *135*, e202302979. [CrossRef]
56. Younis, S.; Kim, K.-H. Heterogeneous Photocatalysis Scalability for Environmental Remediation: Opportunities and Challenges. *Catalysts* **2020**, *10*, 1109. [CrossRef]
57. Zhang, F.; Wang, X.; Liu, H.; Liu, C.; Wan, Y.; Long, Y.; Cai, Z. Recent Advances and Applications of Semiconductor Photocatalytic Technology. *Appl. Sci.* **2019**, *9*, 2489. [CrossRef]
58. Ngulube, K.F.; Abdelhaleem, A.; Osman, A.I.; Peng, L.; Nasr, M. Advancing Sustainable Water Treatment Strategies: Harnessing Magnetite-Based Photocatalysts and Techno-Economic Analysis for Enhanced Wastewater Management in the Context of SDGs. *Environ. Sci. Pollut. Res.* **2024**, *32*, 28159–28195. [CrossRef]
59. Huang, S.; Fan, Z.-P.; Wang, X. Optimal Financing and Operational Decisions of Capital-Constrained Manufacturer under Green Credit and Subsidy. *J. Ind. Manag. Optim.* **2021**, *17*, 261–277. [CrossRef]
60. Tan, W.; Huang, Y.; Chen, X.H.; Gatto, A. Green Credit Policy and Energy Consumption Intensity in China: Firm-Level Evidence. *J. Environ. Manag.* **2024**, *373*, 123664. [CrossRef]
61. Huang, S.; Fan, Z.-P.; Wang, N. Green Subsidy Modes and Pricing Strategy in a Capital-Constrained Supply Chain. *Transp. Res. Part E Logist. Transp. Rev.* **2020**, *136*, 101885. [CrossRef]
62. Xi, B.; Jia, W. Research on the Impact of Carbon Trading on Enterprises' Green Technology Innovation. *Energy Policy* **2025**, *197*, 114436. [CrossRef]
63. Chen, Z.; Zhang, Y.; Wang, H.; Ouyang, X.; Xie, Y. Can Green Credit Policy Promote Low-Carbon Technology Innovation? *J. Clean. Prod.* **2022**, *359*, 132061. [CrossRef]
64. Muthukumar, C.; Saginala, P.; Changmai, M.; Prakash Kumar, B.G. Natural Sunlight-Driven Enhanced Abatement of Real Resin Industry Wastewater Using Sludge-Derived Photocatalyst: Potential to Generate Carbon Credits. *J. Environ. Chem. Eng.* **2023**, *11*, 111014. [CrossRef]
65. Shokri, A.; Shokri, A.; White, D.; Gelski, R.; Goldberg, Y.; Harrison, S.; Rashidi, T.H. EnviroCoin: A Holistic, Blockchain Empowered, Consensus-Based Carbon Saving Unit Ecosystem. *Sustainability* **2022**, *14*, 6979. [CrossRef]
66. Yang, R.; Tang, W.; Zhang, J. Technology Improvement Strategy for Green Products under Competition: The Role of Government Subsidy. *Eur. J. Oper. Res.* **2021**, *289*, 553–568. [CrossRef]

67. Sinfield, J.V.; Ajmani, A.; McShane, W. Strategic Roadmapping to Accelerate and Risk-Mitigate Enabling Innovations: A Generalizable Method and a Case Illustration for Marine Renewable Energy. *Technol. Forecast. Soc. Change* **2024**, *209*, 123761. [CrossRef]
68. Li, Y.; Su, X.; Bai, M. A Stochastic Dynamic Programming Model for the Optimal Policy Mix of the Carbon Tax and Decarbonization Subsidy. *J. Environ. Manag.* **2024**, *353*, 120242. [CrossRef] [PubMed]
69. Koval, V.; Laktionova, O.; Udovychenko, I.; Olczak, P.; Palii, S.; Prystupa, L. Environmental Taxation Assessment on Clean Technologies Reducing Carbon Emissions Cost-Effectively. *Sustainability* **2022**, *14*, 14044. [CrossRef]
70. Tchorzewska, K.B.; Rio, P.D.; Garcia-Quevedo, J.; Martinez-Ros, E. Carrot First, Stick Second? Environmental Policy-Mix Sequencing and Green Technologies. *Technol. Forecast. Soc. Change* **2025**, *210*, 123835. [CrossRef]
71. Theyel, G.; Tucci, C. Risk-Sharing and Its Role in Manufacturer's Innovation. *Prod. Manuf. Res.* **2024**, *12*, 2296051. [CrossRef]
72. Zhou, Y.; Pan, M.; Zhou, D.K.; Xue, L. Stakeholder Risk and Trust Perceptions in the Diffusion of Green Manufacturing Technologies: Evidence from China. *J. Environ. Dev.* **2018**, *27*, 46–73. [CrossRef]
73. Tan, L.-L.; Wong, V.L.; Phang, S.J. Recent Advances on TiO_2 Photocatalysis for Wastewater Degradation: Fundamentals, Commercial TiO_2 Materials, and Photocatalytic Reactors. In *Handbook of Nanotechnology Applications*; Elsevier: Amsterdam, The Netherlands, 2021; pp. 25–65, ISBN 978-0-12-821506-7.
74. Cherevko, S. Stabilization of Non-Noble Metal Electrocatalysts for Acidic Oxygen Evolution Reaction. *Curr. Opin. Electrochem.* **2023**, *38*, 101213. [CrossRef]
75. Zhang, C.; Wang, L.; Wu, C.-D. Stabilization of Transition Metal Heterojunctions inside Porous Materials for High-Performance Catalysis. *Dalton Trans.* **2023**, *52*, 8834–8849. [CrossRef]
76. Li, S.; Rao, H.; Tang, C.; Bao, T.; She, P.; Qin, J. Recent Advances of Non-Noble Metals Based Plasma Materials in Photocatalysis. *Coord. Chem. Rev.* **2024**, *510*, 215803. [CrossRef]
77. Yao, Y.; Liu, C.; Xiao, C.; Wang, M.; Zhu, Z.; Yang, Y.; Zhou, Y.; Qi, J.; Richards, H.; Li, J. Metamorphoses of Industrial Waste Sludge via Metal Organic Frameworks into Efficient Fenton-like Catalysts. *Chem. Eng. J.* **2025**, *519*, 165620. [CrossRef]
78. Kumar, A.; Sharma, P.; Sharma, G.; Dhiman, P.; Mola, G.T.; Farghali, M.; Rashwan, A.K.; Nasr, M.; Osman, A.I.; Wang, T. Simultaneous Hydrogen Production and Photocatalytic Pollutant Removal: A Review. *Environ. Chem. Lett.* **2024**, *22*, 2405–2424. [CrossRef]
79. Zhou, Y.; Han, J.; Zhou, Y. Synergizing Carbon Trading and Water Management for Urban Sustainability: A City-Level Multi-Objective Planning Framework. *Appl. Energy* **2024**, *359*, 122637. [CrossRef]
80. Hangai, B.; Ortega, P.; Simoes, A.Z.; Alves, F.; Longo, E.; Zirpoli Simões, A. Enhancing Photocatalytic Efficiency Through Silver Modification of Sodium and Hydrogen Titanate Nanostructures. *Phys. B Condens. Matter* **2024**, *715*, 417550. [CrossRef]
81. Niu, Y.; Shi, Q.; Peng, T.; Cao, X.; Lv, Y. Research Progress on the Synthesis of Nanostructured Photocatalysts and Their Environmental Applications. *Nanomaterials* **2025**, *15*, 681. [CrossRef] [PubMed]
82. Alagarsamy, V.; Venkatesh, N.; Roshan, S.A.; Pandurengan, S.; Gnanasekaran, L.; Viswanathan, K.; Murugadoss, G. NiS-ZnS Quantum Dots as Visible-Light Photocatalysts for Enhanced Dye Degradation in Sustainable Wastewater Treatment. *Chem. Phys. Impact* **2025**, *11*, 100912. [CrossRef]
83. Ding, H.; Wang, H.; Huang, G.; Zhu, Y.; Zhang, L.; Zhang, X.; Zhou, M.; Wang, Q.; Li, X.; Xu, Q.; et al. Assessing the Wastewater Reclaim System Consisted of Wastewater Plant—Hybrid Constructed Wetland—Ultra Filtration and Reverse Osmosis in a Chemical Industrial Park, a Multi-Criteria Decision-Making Analysis. *Sci. Total Environ.* **2024**, *926*, 171942. [CrossRef]
84. Zhang, Y.; Wu, Q.; Ren, H.; Li, Q.; Zhou, W. A Multi-Agent Distributed Electricity-Carbon Shared Trading Strategy Considering Regional Carbon Inclusion. *Renew. Energy* **2025**, *239*, 122075. [CrossRef]
85. Li, X.; Yu, Y.; Pan, J.; Bhuiyan, M.A. Can Carbon Emission Trading Improve Regional Eco-Efficiency? Based on the Environmental Innovation Perspective. *Environ. Sci. Pollut. Res.* **2024**, *31*, 31081–31096. [CrossRef] [PubMed]
86. Ganthavee, V.; Trzcinski, A.P. Artificial Intelligence and Machine Learning for the Optimization of Pharmaceutical Wastewater Treatment Systems: A Review. *Environ. Chem. Lett.* **2024**, *22*, 2293–2318. [CrossRef]
87. Hussain, C.G.; Keçili, R.; Hussain, C.M. Future of Analytical Chemistry with Green Miniaturized Technologies. In *Comprehensive Analytical Chemistry*; Elsevier: Amsterdam, The Netherlands, 2025; Volume 109, pp. 507–537. ISBN 978-0-443-23980-9.
88. Martini, S.; Roni, K.A. The Existing Technology and the Application of Digital Artificial Intelligent in the Wastewater Treatment Area: A Review Paper. *J. Phys. Conf. Ser.* **2021**, *1858*, 012013. [CrossRef]
89. Pandey, A.K.; Reji Kumar, R.; Kalidasan, B.; Laghari, I.A.; Samykano, M.; Kothari, R.; Abusorrah, A.M.; Sharma, K.; Tyagi, V.V. Utilization of Solar Energy for Wastewater Treatment: Challenges and Progressive Research Trends. *J. Environ. Manag.* **2021**, *297*, 113300. [CrossRef]
90. Chen, J.; Hu, L.; Chen, Q.; Yang, T.; Yi, C. Hotspots and Trends in Solar-Driven Interfacial Evaporation Technology Based on Bibliometric Management and Analysis. *Surf. Interfaces* **2024**, *46*, 104184. [CrossRef]
91. Evro, S.; Oni, B.A.; Tomomewo, O.S. Global Strategies for a Low-Carbon Future: Lessons from the US, China, and EU's Pursuit of Carbon Neutrality. *J. Clean. Prod.* **2024**, *461*, 142635. [CrossRef]

92. Chen, J.; Xie, F.; Inna, S.; Liu, B.; Luo, H. Breaking Barriers, Boosting Green: Artificial Intelligence and Green Transformation in Cities. *Sustain. Cities Soc.* **2025**, *130*, 106626. [CrossRef]
93. Zhang, X.; Fan, Y.; Hao, T.; Chen, R.; Zhang, T.; Hu, Y.; Li, D.; Pan, Y.; Li, Y.-Y.; Kong, Z. Insights into Current Bio-Processes and Future Perspectives of Carbon-Neutral Treatment of Industrial Organic Wastewater: A Critical Review. *Environ. Res.* **2024**, *241*, 117630. [CrossRef]
94. Tapia-Tlatelpa, T.; Buscio, V.; Trull, J.; Sala, V. Performance Analysis and Methodology for Replacing Conventional Lamps by Optimized LED Arrays for Photocatalytic Processes. *Chem. Eng. Res. Des.* **2020**, *156*, 456–468. [CrossRef]
95. Wang, D.; Mueses, M.A.; Márquez, J.A.C.; Machuca-Martínez, F.; Grčić, I.; Peralta Muniz Moreira, R.; Li Puma, G. Engineering and Modeling Perspectives on Photocatalytic Reactors for Water Treatment. *Water Res.* **2021**, *202*, 117421. [CrossRef]
96. Jo, W.-K.; Tayade, R.J. New Generation Energy-Efficient Light Source for Photocatalysis: LEDs for Environmental Applications. *Ind. Eng. Chem. Res.* **2014**, *53*, 2073–2084. [CrossRef]
97. Kane, A.; Assadi, A.A.; El Jery, A.; Badawi, A.K.; Kenfoud, H.; Baaloudj, O.; Assadi, A.A. Advanced Photocatalytic Treatment of Wastewater Using Immobilized Titanium Dioxide as a Photocatalyst in a Pilot-Scale Reactor: Process Intensification. *Materials* **2022**, *15*, 4547. [CrossRef]
98. Kubiak, A. A Scalable IoT-Controlled Photocatalytic System for Pharmaceutical Removal in Real Wastewater Treatment Applications. *Chem. Eng. J.* **2025**, *518*, 164709. [CrossRef]
99. Baaloudj, O.; Badawi, A.K.; Kenfoud, H.; Benrighi, Y.; Hassan, R.; Nasrallah, N.; Assadi, A.A. Techno-Economic Studies for a Pilot-Scale $Bi_{12}TiO_{20}$ Based Photocatalytic System for Pharmaceutical Wastewater Treatment: From Laboratory Studies to Commercial-Scale Applications. *J. Water Process Eng.* **2022**, *48*, 102847. [CrossRef]
100. Malato, S.; Fernández-Ibáñez, P.; Maldonado, M.I.; Blanco, J.; Gernjak, W. Decontamination and Disinfection of Water by Solar Photocatalysis: Recent Overview and Trends. *Catal. Today* **2009**, *147*, 1–59. [CrossRef]
101. Acevedo, A.; Carpio, E.A.; Rodríguez, J.; Manzano, M.A. Disinfection of Natural Water by Solar Photocatalysis Using Immobilized TiO_2 Devices: Efficiency in Eliminating Indicator Bacteria and Operating Life of the System. *J. Sol. Energy Eng.* **2012**, *134*, 011008. [CrossRef]
102. Pu, Y.; Jia, L.; Huang, Q.; Tang, X.; Rodriguez, P.; Huang, L. Investigation on the Surface Charge Separation in Pt-Supported Morphology-Related-TiO_2 and Its Effect on Water Splitting. *J. Colloid Interface Sci.* **2023**, *646*, 815–823. [CrossRef] [PubMed]
103. Huang, S.-Y.; Ganesan, P.; Park, S.; Popov, B.N. Development of a Titanium Dioxide-Supported Platinum Catalyst with Ultrahigh Stability for Polymer Electrolyte Membrane Fuel Cell Applications. *J. Am. Chem. Soc.* **2009**, *131*, 13898–13899. [CrossRef]
104. Katz, A.; McDonagh, A.; Tijing, L.; Shon, H.K. Fouling and Inactivation of Titanium Dioxide-Based Photocatalytic Systems. *Crit. Rev. Environ. Sci. Technol.* **2015**, *45*, 1880–1915. [CrossRef]
105. Loh, H.P.; Lyons, J.; White, C.W. *Process Equipment Cost Estimation, Final Report*; DOE/NETL--2002/1169; EG&G Technical Services, Inc.: Morgantown, WV, USA, 2002; p. 797810.
106. Pelayo, D.; Rivero, M.J.; Santos, G.; Gómez, P.; Ortiz, I. Techno-Economic Evaluation of UV Light Technologies for the Simultaneous Disinfection and Water Remediation. *SSRN J.* **2022**, *868*, 161376. [CrossRef]
107. Mei, J.; Gao, X.; Zou, J.; Pang, F. Research on Photocatalytic Wastewater Treatment Reactors: Design, Optimization, and Evaluation Criteria. *Catalysts* **2023**, *13*, 974. [CrossRef]
108. Hirth, L.; Steckel, J.C. The Role of Capital Costs in Decarbonizing the Electricity Sector. *Environ. Res. Lett.* **2016**, *11*, 114010. [CrossRef]
109. Ding, Y.; Zheng, H.; Li, J.; Zhang, S.; Liu, B.; Ekberg, C.; Jian, Z. Recovery of Platinum from Spent Petroleum Catalysts: Optimization Using Response Surface Methodology. *Metals* **2019**, *9*, 354. [CrossRef]

Disclaimer/Publisher's Note: The statements, opinions and data contained in all publications are solely those of the individual author(s) and contributor(s) and not of MDPI and/or the editor(s). MDPI and/or the editor(s) disclaim responsibility for any injury to people or property resulting from any ideas, methods, instructions or products referred to in the content.